การพัฒนาฟิล์มบรรจุภัณฑ์จากพลาสติกชีวภาพ/ดินเหนียว นาโนคอมโพสิต

นายภูมิ บุญเฟื่อง

วิทยานิพนธ์นี้เป็นส่วนหนึ่งของการศึกษาตามหลักสูตรปริญญาวิศวกรรมศาสตรมหาบัณฑิต
สาขาวิชาวิศวกรรมเคมี ภาควิชาวิศวกรรมเคมี
คณะวิศวกรรมศาสตร์ จุฬาลงกรณ์มหาวิทยาลัย
ปีการศึกษา 2554

DEVELOPMENT OF PACKAGING FILM FROM BIOPLASTIC/CLAY NANOCOMPOSITES

Mr. Poom Boonfaung

A Thesis Submitted in Partial Fulfillment of the Requirements
for the Degree of Master of Engineering Program in Chemical Engineering
Department of Chemical Engineering
Faculty of Engineering
Chulalongkorn University
Academic Year 2011

Thesis Title	DEVELOPMENT OF PACKAGING FILM FROM BIOPLASTIC/CLAY NANOCOMPOSITES
By	Mr. Poom Boonfaung
Field of Study	Chemical Engineering
Thesis Advisor	Assistant Professor Anongnat Somwangthanaroj, Ph.D.

Accepted by the Faculty of Engineering, Chulalongkorn University in Partial Fulfillment of the Requirements for the Master's Degree

……………………………… Dean of the Faculty of Engineering
(Associate Professor Boonsom Lerdhirunwong, Dr.Ing.)

THESIS COMMITTEE

……………………………… Chairman
(Associate Professor Tharathon Mongkhonsi, Ph.D.)

……………………………… Thesis Advisor
(Assistant Professor Anongnat Somwangthanaroj, Ph.D.)

……………………………… Examiner
(Associate Professor ML. Supakanok Thongyai, Ph.D.)

………………………………. External Examiner
(Assistant Professor Wanchai Lerdwijitjarud, Ph.D.)

ภูมิ บุญเฟื่อง : การพัฒนาฟิล์มบรรจุภัณฑ์จากพลาสติกชีวภาพ/ดินเหนียว นาโนคอมโพสิต (DEVELOPMENT OF PACKAGING FILM FROM BIOPLASTIC/CLAY NANOCOMPOSITES) อ. ที่ปรึกษาวิทยานิพนธ์หลัก: ผศ.ดร. อนงค์นาฏ สมหวังธนโรจน์, 109 หน้า.

ในงานวิจัยนี้ฟิล์มพอลิแลคติก แอซิด (PLA) ถูกเตรียมขึ้นด้วยวิธีการขึ้นรูปแบบเป่ากลวงโดยใช้เครื่องอัดรีดชนิดสกรูคู่ การวิจัยแบ่งเป็น 2 ส่วน ส่วนแรกศึกษาอิทธิพลของชนิดและปริมาณของสารเสริมสภาพพลาสติกซึ่งสารเสริมสภาพพลาสติกถูกใช้ในการเพิ่มความยืดหยุ่นของ PLA ต่อสมบัติทางความร้อน สมบัติทางกล และสมบัติการป้องกันการซึมผ่านของแก๊สของฟิล์มเป่า PLA ที่ถูกปรับสภาพด้วยสารเสริมสภาพพลาสติก จากผล DSC และ DMA พบว่าสารเสริมสภาพพลาสติกทุกชนิดสามารถเข้าได้ดีกับ PLA ที่ 5 เปอร์เซ็นต์โดยน้ำหนักและสารเสริมสภาพพลาสติกส่งผลให้ระดับในการเกิดผลึกของ PLA เพิ่มขึ้น นอกจากนี้การทดสอบแรงดึง พบว่าพอลิโพรพิลีน ไกลคอล, PPG(1200) ที่ 5 เปอร์เซ็นต์โดยน้ำหนักเป็นสารเสริมสภาพพลาสติกที่เหมาะสมกับ PLA ซึ่งสามารถสังเกตจากการค่าเปอร์เซ็นต์การยืดตัวก่อนขาดเพิ่มขึ้นประมาณ 45 เท่า ส่วนที่สองศึกษาอิทธิพลของชนิดของสารลดแรงตึงผิวและปริมาณของดินเหนียวที่ปรับสภาพด้วยสารลดแรงตึงผิวต่อสมบัติของฟิล์มเป่า PLA/ดินเหนียวนาโนคอมโพสิต จากผล XRD พบว่าระยะห่างระหว่างชั้นของดินเหนียวที่ปรับสภาพด้วยสารลดแรงตึงผิวเพิ่มขึ้นเมื่อเปรียบเทียบกับดินเหนียวบริสุทธิ์ นอกจากนี้ฟิล์ม PLA/ดินเหนียวที่ปรับสภาพด้วย trimethyl tallow quaternary ammonium chloride (PLA/MMT/M_3T films) มีการกระจายตัวของดินเหนียวและการส่องผ่านของแสงดีกว่าฟิล์ม PLA/ดินเหนียวที่ปรับสภาพด้วย tallow bis(2-hydroxyethyl) amine (PLA/MMT/HT$(OH)_2$ films) นอกจากนี้ผลของ DSC และ DMA แสดงว่าฟิล์ม PLA/MMT/HT$(OH)_2$ ให้ระดับในการเกิดผลึกมากกว่าของฟิล์ม PLA/MMT/M_3T สำหรับสมบัติทางกลฟิล์ม PLA/MMT/M_3T มีค่าเปอร์เซ็นต์การยืดตัวก่อนขาดมากกว่าของฟิล์ม PLA/MMT/HT$(OH)_2$ และพบว่าที่ 3 เปอร์เซ็นต์โดยน้ำหนักของดินเหนียวที่ปรับสภาพด้วยสารลดแรงตึงผิวมีความเหมาะสมกับ PLA ที่ถูกปรับสภาพด้วยสารเสริมสภาพพลาสติก นอกจากนี้ฟิล์ม PLA/MMT/HT$(OH)_2$ แสดงการซึมผ่านของไอน้ำมากกว่า (6.19 %) ของฟิล์ม PLA/MMT/M_3T แต่การซึมผ่านของออกซิเจนต่ำกว่า (7.94 %) เมื่อเทียบกับฟิล์ม PLA/MMT/M_3T

ภาควิชา……วิศวกรรมเคมี……. ลายมือชื่อนิสิต…………………………………………
สาขาวิชา……วิศวกรรมเคมี……. ลายมือชื่อ อ.ที่ปรึกษาวิทยานิพนธ์หลัก…………………..
ปีการศึกษา……2554……….

5270448621 : MAJOR CHEMICAL ENGINEERING

KEYWORDS: POLYLACTIC ACID/PLASTICIZERS/SURFACTANTS/CLAY

POOM BOONFAUNG: DEVELOPMENT OF PACKAGING FILM FROM BIOPLASTIC/CLAY NANOCOMPOSITES. ADVISOR: ASST. PROF. ANONGNAT SOMWANGTHANAROJ, Ph.D., 109 pp.

In this study, polylactic acid (PLA) films were prepared via twin screw extruder attached with blown film die. The research consisted of two parts. The first part concentrates on studying the effect of types and loading of plasticizer, in which they were used to increase the flexibility of PLA, on thermal, mechanical and gas barrier properties of plasticized PLA blown films. From DSC and DMA results, 5 wt% of all plasticizers were compatible with PLA and it affected degree of crystallinity of PLA increased. In addition, tensile tests indicated that polypropylene glycol, PPG(1200) at 5 wt% was a suitable plasticizer for PLA which can be observed from an increase in elongation at break approximately 45 times. The second part focuses on the effect of surfactant types and organoclay loading on properties of PLA/clay nanocomposite blown films. From XRD result, interlayer spacing of organoclay increased compared with that of pristine clay. Furthermore, film of PLA/montmorillonite modified by trimethyl tallow quaternary ammonium chloride (PLA/MMT/M_3T films) showed better clay dispersion and higher transmittance of light than film of PLA/montmorillonite modified by tallow bis(2-hydroxyethyl) amine (PLA/MMT/HT$(OH)_2$ films). Furthermore, from DSC and DMA results, PLA/MMT/HT$(OH)_2$ films gave higher degree of crystallinity than PLA/MMT/M_3T films. For mechanical properties, PLA/MMT/M_3T films exhibited higher elongation at break than PLA/MMT/HT$(OH)_2$ films and 3 wt% of organoclay showed optimum properties when added into with plasticized PLA. In addition, PLA/MMT/HT$(OH)_2$ films showed higher water vapor permeation (6.19 %) but lower oxygen permeation (7.94 %) compared to PLA/MMT/M_3T films.

Department: Chemical Engineering Student's Signature ....

Field of Study: Chemical Engineering Advisor's Signature ....

Academic Year: 2011

ACKNOWLEDGEMENTS

I would like to express a sincere appreciation to my advisor, Assistant Professor Dr. Anongnat Somwangthanaroj, for her kindness, guidance and helping me throughout my research thesis and editing of this thesis.

I am great appreciate to the chairman, Associate Professor Dr. Tharathon Mongkhonsi and committee members, Associate Professor ML Dr. Supakanok Thongyai and Assistant Professor Dr. Wanchai Lerdwijitjarud for giving some advice that is useful for my research.

I would especially like to thank to Kunimine Industrial Company and Akzo Nobel, Thailand for supporting materials which were clay (Na-montmorillonite) and surfactant respectively in this research.

Furthermore, I sincerely thank Thailand Research Fund (TRF-MASTER RESEARCH GRANTS) and Mahachai Plastic Factory for financial supports in my research.

Moreover, I thank everyone in the Polymer Engineering Research Laboratory, Department of Chemical Engineering, Chulalongkorn University, for taking discussion, giving some advice and friendly encouragement. Besides, I would like to thank Mr. Puwanut Wasutchanon and Mr. Chavakorn Samthong for their kindly helping process blown film, exchanging an opinion together with editing my thesis and answered my questions.

Finally, I would like to express a sincere gratitude to the members of my family for their encouragement, and support throughout my entire study.

CONTENTS

PAGE

PAGE

LIST OF TABLES

TABLE **PAGE**

TABLE **PAGE**

TABLE **PAGE**

LIST OF FIGURES

FIGURE **PAGE**

FIGURE **PAGE**

LIST OF ABBREVIATIONS

PLA	Polylactic acid
PPG	Polypropylene glycol
PEPG	Poly (ethylene glycol-co-propylene glycol)
DOP	Dioctyl phthalate
TBC	Tributyl citrate
DSC	Diffetrential scanning calorimeter
XRD	X-ray diffraction
DMA	Dynamic mechanical analysis
UV-vis	Ultraviolet-visible spectrometer
T_g	Glass transition temperature
T_c	Cold crystallization temperature
T_m	Melting temperature
E'	Storage modulus
MMT	Montmorillonite
M_3T	Trimethyl tallow quaternary ammonium chloride
$HT(OH)_2$	Tallow bis(2-hydroxyethyl) amine

CHAPTER I

INTRODUCTION

1.1 General Introduction

Plastics are extensively used in almost daily activities such as the plastic packaging bags produced from polyethylene and polypropylene. Plastics have several advantages such as light weight, no rust, low cost of fabrication and simple processability; thus, it can be utilized in the large areas which increase the production and consumption rate. However, the products from these polymers cause environmental pollution because the nature of plastic needs long time to be decomposed, possibly up to hundreds of years and difficult to eliminate after uses. The currently used methods to manage plastic wastes are to eliminate it via burial, incineration and recycle but it is still inefficient as expected. Those problems are the important factor to take the bioplastic and renewable materials to replace the conventional petroleum based plastics. Many research and development on biodegradable plastics such as aliphatic polyesters have been increasingly carried out. Biodegradable plastics are decomposed by the action of enzymes or microorganisms. Among the biodegradable aliphatic polyesters, polylactic acid (PLA) has been aggressively investigated and developed.

PLA has attracted both industries and research institutions. It is one of the biopolymer whose properties are comparable with the commercial plastic such as poly (ethylene terephthalate) (PET). Production of PLA is derived from annually renewable resources such as corn starch, cassava starch or sugarcanes. PLA exhibits good properties such as biodegradability, heat resistance, transparency, good mechanical properties and processability, causing it to be used in many packaging applications. The important requirement for packaging materials is high tensile strength, ductility, flexibility, transparency and good barrier properties. However, PLA is still limited for its application because of its price, brittleness, rigidity and low crystallization rate. Therefore, plasticizers can be used to increase the flexibility of PLA for packaging applications such as, packaging films, wrap films, stretch films and agricultural mulch films. Moreover, the addition of nanoclay into PLA matrix is also a method to enhance its mechanical, thermal and gas barrier properties.

Attempt has been made to improve the processability and flexibility of PLA by mixing with plasticizer. The choice of plasticizers to be used as modifiers for PLA is non toxic for food contact which can be considered as plasticizing agents in food packaging films. For a low molecular weight plasticizer, an important demand is miscible with PLA and stable at high temperature used during processing, thus creating a homogeneous mixing. Plasticized PLA should be stable for anytime because the removal of plasticizer to the surface could be contamination of the food or beverage in contact with the packaging or may possibly recover the primary brittleness of neat PLA.

Recently, polymer/clay nanocomposites, in which the clays are intercalated or exfoliated into polymer matrix, have been more interesting in the industry to improve a polymer as it increases the various properties of the polymer. Polymer/clay nanocomposites have many advantages compared to the traditional microcomposites, such as lower loading of clay, lower density, improved transparency and increased barrier properties.

Clay can be very well disperse in PLA matrix by the ion exchange reactions with cationic surfactants such as alkylammonium, in which the surfactant will lower the surface attraction of the clay and results in increased interlayer spacing.

Montmorillonite is one type of clay, which is widely used, whose category is in the smectite. PLA/clay nanocomposite exhibits great improvement of performances more than neat polymer such as high strength, decreased gas permeability, high heat resistance and increased biodegradability.

The main objective of this study is to improve and modify packaging film produced from PLA by the addition of plasticizers and nanoclay which will enhance ductility, flexibility, strength and heat resistance of the packaging films. The study is mainly focused on the miscibility, meachnical, thermal and gas barrier properties of additived PLA blown films.

1.2 Objectives

1. To study the effect of chemical structure and molecular weight of plasticizers as well as the amounts of plasticizer on the mechanical and thermal properties of plasticized PLA blown films
2. To study the effect of surfactant’s structure on the degree of clay dispersion in PLA/clay nanocomposite films

3. To investigate the effect of organoclay loading on mechanical, thermal and gas barrier properties of PLA/clay nanocomposite films

1.3 Scopes of the research

1. Choose the suitable plasticizers blended with PLA
    - Polypropylene glycol (PPG) MW 1200 and 2000 g/mol
    - Poly (ethylene glycol-co-propylene glycol) (PEPG)
    - Dioctyl phthalate (DOP)
    - Tributyl citrate (TBC)
    - Adipic acid, sebacic acid and dodecanedioic acid
2. Investigate the optimum conditions to obtain the plasticized PLA blown films, containing 3%, 5% and 7% by weight of plasticizer
3. Study the effect of type of surfactants; i.e, trimethyl tallow quaternary ammonium chloride and tallow bis(2-hydroxyethyl)amine, on the mechanical, thermal and gas barrier properties of PLA/clay nanocomposite films
4. Investigate the optimum conditions for PLA/clay nanocomposite films, containing 1%, 3% and 5% by weight of organoclay

CHAPTER II

THEORY

2.1 Polylactic acid

2.1.1 Lactic acid

PLA is a biodegradable thermoplastic in family of aliphatic polyesters, which it is derived from a fermentation process using renewable resources such as corn starch or sugar beets [1]. The PLA will also rapidly degrade in the environment. Furthermore, the by-products have very low toxicity and eventually being converted to carbon dioxide and water [2].

Lactic acid (2-hydroxypropionic acid) is the basic building block for Polylactic acid (PLA). It is a highly water-soluble, three-carbon chiral acid that can be naturally occurred. The lactic acid has two optical isomers L and D-lactic acid [2-5]. L-lactic acid is the natural and most common form of the acid, but D-lactic acid can also be produced by microorganisms. D-lactic acid is impurity and acts much like co-monomers in other polymers such as polyethylene terephthalate (PET) or polyethylene (PE) [2]. D-lactic acid units are incorporated into L-PLA to optimize the crystallization kinetics for specific fabrication processes and applications. The chemical structure of the D-Lactic acid and L-Lactic acid is displayed in Figure 2.1.

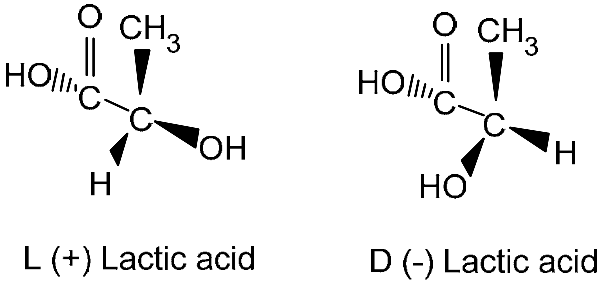

Figure 2.1 Lactic acid optical isomers

2.1.2 Synthesis of polylactic acid

PLA can be prepared by both the direct condensation of lactic acid and the ring-opening polymerization of the cyclic lactide dimer [1, 2], as shown in Figure 2.2. The direct condensation route is an equilibrium reaction. So, this system is difficult to eliminate the water. This method cannot be achieved with the high molecular weight. Most study has focused on the ring-opening polymerization of lactide whose mechanism does not generate additional water; hence, a wide range of molecular weights is accessible [2].

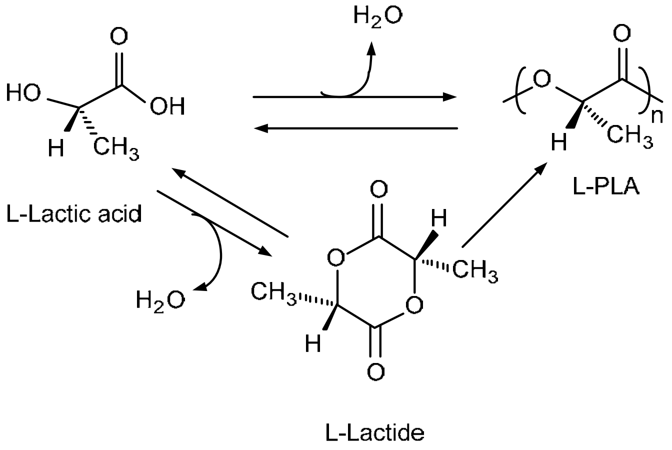

Figure 2.2 Polymerization routes to polylactic acid

The process to obtain PLA is displayed in Figure 2.3, in which lactic acid is produced by fermentation of dextrose, followed by a continuous condensation reaction of aqueous lactic acid to produce low molecular weight PLA prepolymer. Next, the low molecular weight oligomers are converted into a mixture of lactide stereoisomers using a catalyst to enhance the rate and selectivity of the intramolecular cyclization reaction. The molten lactide mixture is then purified by vacuum distillation. Finally, high polymer of PLA is produced using an organo tin-catalyzed, ring opening lactide polymerization in the melt. After the polymerization is completed, any remaining monomer is removed under vacuum and recycled to the beginning of the process [2].

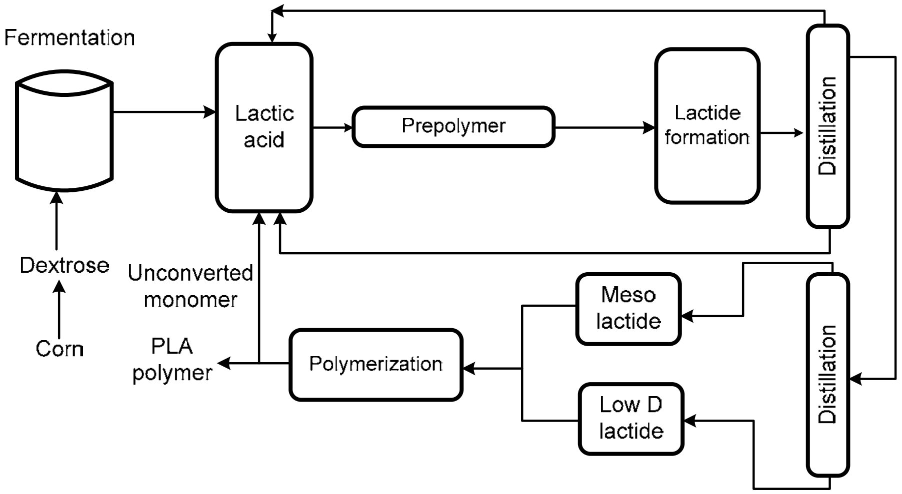

Figure 2.3 Process to prepare polylactic acid [2]

2.1.3 Thermal properties of PLA

PLA has a crystallinity of around 37%, a glass transition temperature (T_g) between 50-80 ^oC and a melting temperature (T_m) between 173-178 ^oC. The T_g of PLA depends on both the molecular weight and the optical isomers of the polymer.

Furthermore, it is also dependent on the thermal history of the polymer. The T_m of PLA is also a function of its optical purity. The maximum practical obtainable T_m for stereochemically neat PLA is around 180 ^oC. In the solid state, PLA can be either amorphous or semicrystalline, depending on the stereochemistry and thermal history [1].

2.1.4 Degradation of PLA

PLA products will rapidly degrade in both aerobic and anaerobic composting conditions and disintegrate within weeks to months under conditions of high temperature and high humidity. The degradation of PLA occurs by a two-step process. The primary mechanism of degradation is hydrolysis in which the high molecular weight polyester chains hydrolyze to lower molecular weight oligomers followed by bacterial attack on the fragmented residues. The rate of hydrolysis is accelerated by acids or bases and also depends on moisture content and temperature [1, 2].

2.1.5 Applications of PLA

PLA is an eco-friendly polymer that is ideally suited for many applications in the environment such as agricultural mulch films and bags. However, PLA is still limited for its application because of its brittleness and rigidity. Thus, PLA was improved with various methods such as blending, copolymerization, and the addition of impact-modified products which will further expand the applications.

2.2 Modification of PLA

2.2.1 Mixing

The mixing method is widely used to improve the polymer’s properties between an original form of polymer and other forms or plasticizer. Fluid forms are included with a solution and molten blended into one form as a polymer blend, which has the combination of each property from those forms. However, its mixing process is hardly occurred, so the polymer blend from process is not a real fluid solution. Also, it is found that the liquid form of one polymer will disperse into the continuous matrix of another polymer, and it must distribute equally. Otherwise, its final product will be defective and leads to lower mechanical properties of the polymer blend than the neat polymer. Therefore, it should be considered that the compatibility of each polymer mixture as some of them may not be blended due to the difference in chain structures. Moreover, the energy factor, including the molecular integration or the polymer chain structure, may affect the forms of polymers in mixing process since it will absorb the thermal energy of each polymer [6].

2.2.2 Plasticizers

Plasticizer is an additive added in the polymer in order to enhance the processability, flexibility and stretchability as it is able to reduce the glass transition temperature of polymer without changing its original chemistry characteristic.

Plasticizers are used in various polymers. The plasticizers are used with the polymers that are brittle as it needs a high temperature in processing. Therefore, adding small amount of plasticizers will easier its processing at the low temperature and obtained polymers are more flexible.

2.2.2.1 Theory and effect of plasticizers [6, 7]

Lubrication Theory

Generally, plasticizers have worked as a lubricant which theirs molecules are inserted between molecules of polymer to extend the distances of polymer without any chemical reaction. As a result, the attraction of each molecule of polymer is lowered and the polymer with rigidity and brittleness characteristics can transform to flexibility and softness. Moreover, they reduce the viscosity of the liquid polymer.

Solution Theory

Basically, plasticizers which are in a liquid form with a high boiling point can be combined into one form with polymer and well stick with polymer matrix. Also, plasticizers should not have too high attraction with polymer as their molecules may stick too tight with polymers' molecules. This leads to the difficulty in a molecule's chain movement. This reaction is called anti-plasticization. Therefore, plasticizers' molecules should be able to move in the polymer matrix but should not be combined in the surface of the polymer.

Polarity Theory

From theory, the molecular attractions of plasticizers and polymers should be well stabilized in order to produce stable gel. Therefore, plasticizers must be composed of a polar and non polar group to relate with polarity of the polymer. The polarity of plasticizers depends on functional groups of oxygen, phosphorus, and sulfur.

2.3 Clay

Clay minerals are hydrous alumino-silicates (phyllosilicates). Almost all clays contain two basic components which occur from different arrangements. These two basic building blocks of all clay minerals are the silica tetrahedron and the aluminum octahedron, whose structure are shown in figure 2.4. These tetrahedral and octahedral sheets are variously arranged and modified during mineral formation to create several types of clay minerals. Each type of clay has unique chemical and behavioral properties which arise from the structure of the clay minerals [1, 8].

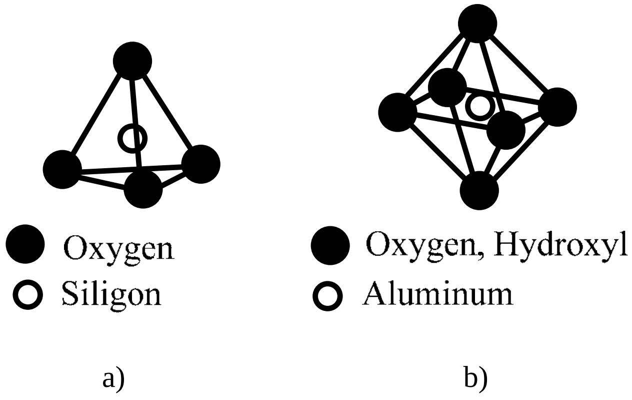

Figure 2.4 a) Silicon-Oxygen Tetrahedron (SiO_4), b) Aluminum Octahedron, Al $(OH)_6^{3-}$

The most well known layered silicate is smectite. Smectite clays have good properties such as low-permeability and expandability. Each layer consists of aluminium or magnesium hydroxide octahedral sheet which was sandwiched between two silicon oxide tetrahedral sheets. The isomorphic substitution of the tetrahedral or octahedral cations, e.g. the substitution of Si^{4+} with Al^{3+} or Al^{3+} with Mg^{2+}, generates negative charges that are counterbalanced by alkali and alkaline earth cations located inside the galleries. In the case of tetrahedral substitution, the negative charge is located on the surface of the silicate layers; thus, the polymer matrices can interact more readily with tetrahedral than with octahedral substituted material [8]. These isomorphic substitutions lead to the net negative charges on the clay structure which must be satisfied by the presence of charge balancing cations such as Ca^{2+} and Na^{+}. These cations between the layers are part of the cation exchange capacity (CEC) of the clay. The definition of cations exchange capacity (CEC) is the number of exchangeable interlayer cations which is usually described as meq/100 g of clay. Smectite clays have CEC values range from 60-120 meq/100 g of clay. Smectite clays can be classified several groups as listed in Table 2.1 [9].

Table 2.1 Species in smectite clay groups [10]

Species	tetrahedrons	octahedrons
Montmorillonite	Si	Al
Beidellite	Si and Al	Al
Nontronite	Si and Al	Fe
Hectorite	Si	Mg and Li
Saponite	Si and Al	Mg

Montmorillonite is considered as a specific smectite mineral, which it has two tetrahedral sheets sandwiching a central octahedral sheet. The layer is thickness of each platelet is around 1 nm and is located on top of each other like the pages of a book. Van der Waals gaps are created between the layers, which show very weak bonding due to various cations between the sheets. Therefore, they exhibit great ability to expand, especially under wet condition [1, 8, 9]. The general structure of montmorillonite is illustrated in Figure 2.5.

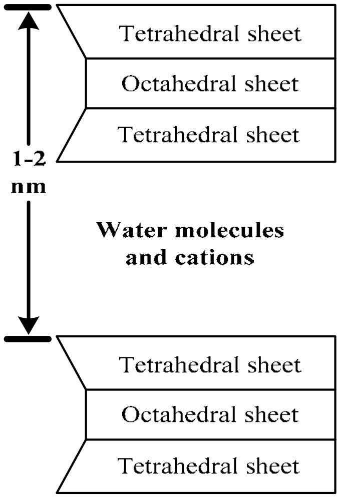

Figure 2.5 Structural scheme of montmorillonite

2.4 Polymer/Clay Nanocomposites

Nanocomposites materials are two phase systems that consist of a polymer matrix and organically modified layered silicate of clay. Nanocomposites exhibit improved several properties such as physical, mechanical, barrier and thermal properties.

2.4.1 Type of Polymer/Clay Nanocomposites

The dispersion of layered silicates in a polymer matrix can be characterized in three types which are shown in Figure 2.6. A phase-separated composite is obtained when the polymer is unable to intercalate between clay layers. Both the intercalated and exfoliated nanocomposites are formed by polymer chains diffuse into space between clay layers or galleries but the number of polymer chains between clay layers of exfoliated nanocomposites is almost continuously variable more than intercalated nanocomposites. In addition, it is individually dispersed in polymer [8, 11].

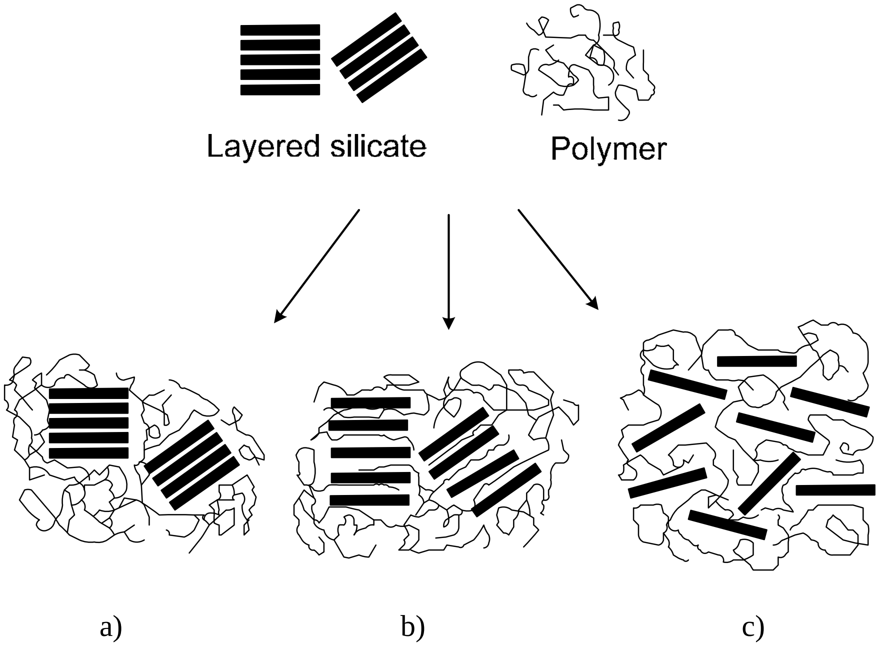

Figure 2.6 Illustration of the three possible types of polymer/clay nanocomposites: a) conventional composites, b) intercalated nanocomposites, c) exfoliated nanocomposites

2.5 Extrusion Process

The extrusion process, which is shown in Figure 2.7, converts thermoplastic pellets into a homogeneous melt at sufficient pressure to allow the melt to flow through a die into a variety of shapes [12]. In this process, the pellets must be conveyed, compressed and melted as they move through the barrel and a die with a steady rate. Between the screw and a die has the screen pack, which can help filter out dirt from polymer matrix. Examples of extruder product are blown film, blown molding and pipe.

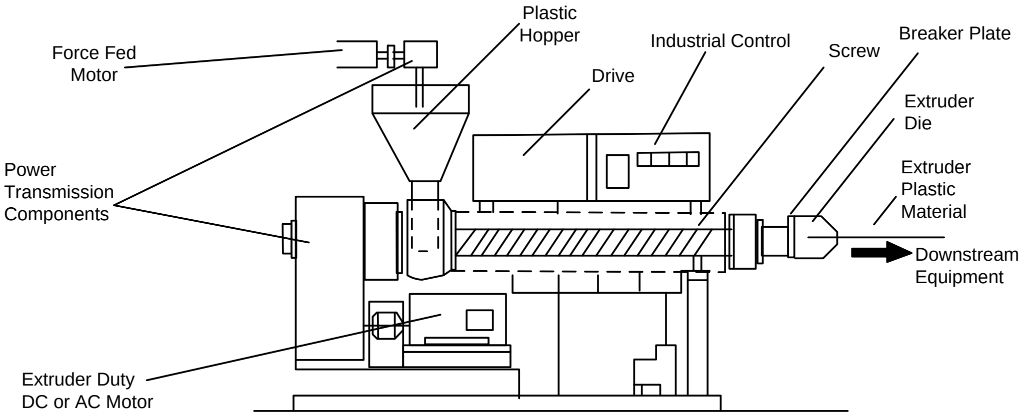

Figure 2.7 Scheme of the extruder

2.5.1 Blown Film Extrusion

Blown film extrusion is another process used to make thermoplastic film, which is produced using an extruder in combination with a blown film die. The blown film line comprising the extruder, die, and blown film is shown in Figure 2.8. In this figure, the molten polymer flows through an annular die to form a bubble or tube that bubble is pulled from the die vertically to nip roll as the bubble is cooled with air. After cooling, two nip rolls will collapse the bubble into two flat layers. Film's width and thickness is controlled by the volume of air in the bubble, the speed of screw and output of the extruder [12].

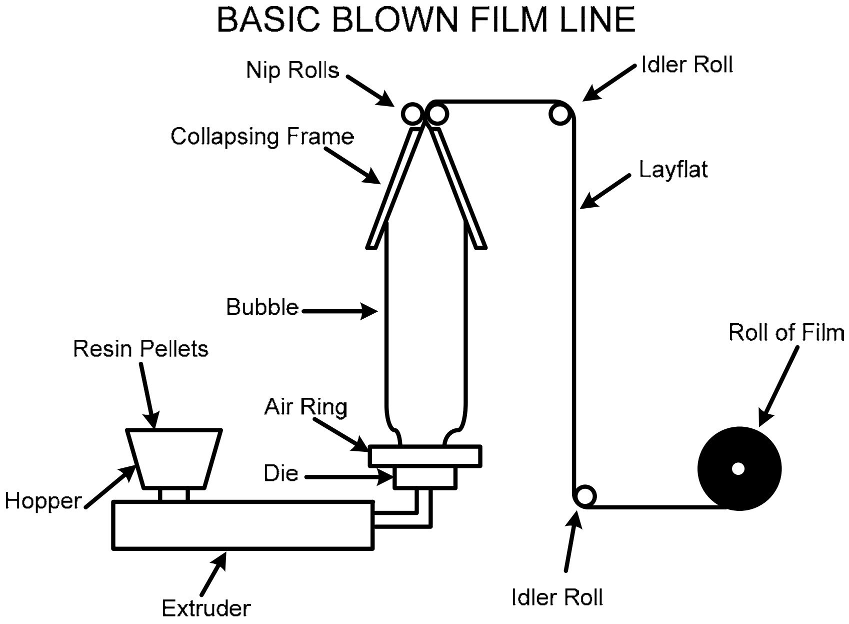

Figure 2.8 Scheme of blown film extrusion

CHAPTER III

LITERATURE REVIEWS

Nowadays, many researchers have studied about the packaging film made from biodegradable plastic. One of biopolymer is Polylactic acid (PLA), but it has the big trouble from PLA film production. PLA film is brittle and rigidity whose properties such as mechanical and thermal properties have to be improved by addition of plasticizers and nanoclay. The main function of plasticizers is to transform polymer from brittleness to soft and flexible. The main function of nanoclay is to increase tensile strength and Young's modulus. In addition, it also increases the stability of temperature. The improvement of PLA depends on type, molecular weight and amount of plasticizer [3-5, 13-15]. Besides, it also depends on number of alkyl chain, length of alkyl chain and amount of surfactant [11, 16-22]. The researches about the processing PLA in compression molding at temperature 170-200 ^{o}C, 0.8-1 mm thick was found that the plasticizer and nanoclay affected thermal, thermo mechanical, mechanical properties as well as morphology of PLA.

From studying the thermal property by differential scanning calorimeter (DSC) of PLA, it was found that the addition of various plasticizer (plasticized PLA), such as dioctyl phthalate (DOP) [15], polypropylene glycol (PPG) [1, 22], poly (ethylene glycol-co-propylene glycol) (PEPG) [5] and tributyl citrate (TBC) [13, 14], when increasing amount of plasticizer, the crystallization temperature (T_c) and melting temperature (T_m) of polymer blend slightly decreased and the glass transition temperature (T_g) dramatically decreased. Furthermore, the addition of TBC 15-20 wt% into PLA, the glass transition temperature decrease about 20-25 ^{o}C when compared with neat PLA (59 ^{o}C) [13, 14] because the chain of plasticized PLA moved more easily [13-15].

Dynamic mechanical analysis (DMA) can be used to study the storage modulus ($E^{/}$), loss modulus ($E^{//}$) and tan δ of the plasticized PLA. Generally, the loss modulus of all of neat PLA which can be well miscible with plasticizer shows only 1 peak [2, 14, 15, 22]. Moreover, the loss modulus of PLA added with high molecular weight of PPG or oligomeric plasticizers shows two peaks at the temperature of 50 ^{o}C and below 0 ^{o}C. The partial phase separation was occurred [1, 14, 22]. Furthermore, the adding of the large content of low M_W of plasticizer can cause partial phase separation [4].

In addition, morphology of plasticized PLA indicates the phase separation and the mechanism of fracture surface of polymer by means of scanning electron microscopy (SEM). The addition of DOP and PPG over 12.5 percent by weight in neat PLA, phase separation occurs because of the accumulation of plasticizer in amorphous phase of the blend [15, 22]. Besides, the fracture surface of PLA that was added with greater amounts of plasticizer should cause more plastic deformation and result to more increased ductility which will show higher elongation at break [2, 15, 22]. The surface of neat PLA and PLA added with PEPG 5 percent by weight was observed by SEM. Film does not show necking and the fracture surface looks smooth [2] because the amount of plasticizer is insufficient to make PLA to occur plastic deformation [1]. However, the PLA added with PEPG more than 10 percent by weight, the fracture surface of film is rough and the significant stretching of film is observed [2].

The effect of plasticizer on mechanical properties by the tensile testing and notched impact test of plasticized PLA was studied. It was found that increase the amount of plasticizer made the PLA showing more plastic deformation due to lower tensile strength at yield and Young's modulus but the elongation at break increases [1, 2, 13, 15, 22]. However, the addition of small amount of plasticizer does not affect the elongation at break [15]. The tensile strength at yield and Young's modulus of PLA added with DOP 12.5 percent by weight (45 MPa, 1330 MPa) shows the lowest value when compared with that of neat PLA (55 MPa, 1680 MPa) at 18% and 20%, respectively [15]. The elongation at break of PLA added with PEPG 10 percent by weight is 340% which is the highest value when compared with that of neat PLA at 4% which increased by 85 times [2]. From the notched impact test, the impact strength of PLA added with TBC exhibits higher value than that of neat PLA [14].

The addition of nanoclay into PLA matrix is also a factor that have been studied by several researchers in order to improve the properties of PLA such as mechanical, thermal and barrier properties [11, 16-22]. However, surface of clay is relatively more hydrophilic than PLA. Therefore, it has to be organically modified to compatibilize and facilitate its dispersion in PLA. One useful characteristic of clay in smectite group is the cations in the galleries, typically Na^+, Li^+, Ca^{2+}, Fe^{2+} and Mg^{2+} which can be substituted readily through ion exchange with organic cations, by treating the clay with surfactants. The interaction of these small molecules between the layers reduces the forces that hold the stacks together and the resulting modified clays (or organoclays) are more compatible with the PLA [11, 17, 22].

Numerous studies have focused on the effect of the number of alkyl chain of surfactants on the interlayer spacing of organoclay [17, 22]. It was observed that the interlayer spacing of organoclay with single alkyl chain surfactants was lower than those of organoclay with double alkyl chains but those with organoclay with triple alkyl chain showed less expanded interlayer spacing than those with double chain [22]. Furthermore, interlayer spacing of clay also depends on the length of alkyl chain and surfactant loading [17, 19, 22]. When alkyl chain length and surfactant loading increased interlayer spacing of clay was increased; however, no change in the interlayer spacing of clay when mixing PLA with 5 wt% organoclay [19]. Furthermore, organoclay depends on the polarity of polymer matrix. The polar polymer can make clays to disperse in polymer matrix as exfoliation such as Nylon [23], while, nanocomposites of non-polar polymers such as polypropylene and polyethylene show opposite trends [24, 25].

There were many researches that focus on the effect of organoclay contents on mechanical properties including Young’s modulus, tensile strength and elongation at break. It was found that the Young’s modulus and tensile strength of PLA/clay nanocomposites gradually increased with increasing organoclay content because uniform dispersion of the nanoclay produces higher interfacial area and ionic bonds between the nanoclay and PLA [18, 19]. However, organoclay at 5 wt% gave the maximum tensile strength and its value began to decrease when organoclay content is over 5 wt%. It is due to the agglomeration of organoclay above the critical content of clay. However, the elongation at break of the nanocomposites slightly decreased with the increase of organoclay lower than 5 wt% [19].

The thermal property of PLA/clay nanocomposites is also an important factor. Crystallization temperatures (T_c) of nanocomposites were sharper and appeared at much lower temperature than that of neat PLA because the neat PLA exhibits large spherulites, where as the sizes of nanocomposite’s spherulites are significantly smaller. This behavior indicates that the surface of the dispersed organoclay acts as a nucleating agent for PLA crystallization [11]. Besides, it was observed that the nature of the organoclay slightly affect the glass transition temperature (T_g) and melting temperature (T_m) of the PLA matrix [11, 17, 19].

Additionally, a resistance of gas permeation of polymer/clay nanocomposites with a wide range of polymer matrix such as polyethylene [24, 25] and polylactide [11, 18, 20] has been extensive studied. Barrier properties of polymer/clay nanocomposites increased with increasing the organoclay loading. For example, the oxygen permeation of PLA decreased by 36 percentage when organoclay loading approached to 5 wt%. It is due to layered silicates that were dispersed in polymer matrix created a tortuous pathway [11].

The influence of additives affects the better properties of PLA, which result from increase of free space and easy movement of the polymer chain. Furthermore, nanocomposites were hypothesized that the exfoliated structure obtained from melt mixing between PLA with organoclay improved mechanical, thermal and gas barrier properties compared to those of neat PLA.

CHAPTER IV

EXPERIMENTS

4.1 Materials

PLA was supplied by Nature Works, USA. The selected grade, PLA 2002D, is a semi crystalline extrusion material. The used plasticizers were Polypropylene glycol (PPG) molecular weight 1200 and 2000 g/mol, Poly (ethylene glycol-ran-propylene glycol) (PEPG), Dioctyl phthalate (DOP), Adipic acid (C = 6), sebacic acid (C = 10) and dodecanedioic acid (C = 12) which were obtained from Sigma-Aldrich chemical, USA, Tributyl citrate (TBC) was obtained from ACROS organics, USA. Their structures were shown in Figure 4.1.

Na-montmorillonite with cation exchange capacity (CEC) of 91.5 meq/100g (ASTM C 837) of clay was supplied by Kunimine Industrial Co.,Ltd., Japan. The used surfactants were Trimethyl tallow quaternary ammonium chloride, represented by M_3T, and tallow bis(2-hydroxyethyl) amine, represented by $HT(OH)_2$, supplied by Akzo Nobel Co., Ltd., Thailand. Their structures were shown in Figure 4.2.

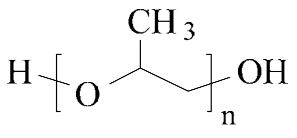

Polypropylene glycol (PPG)

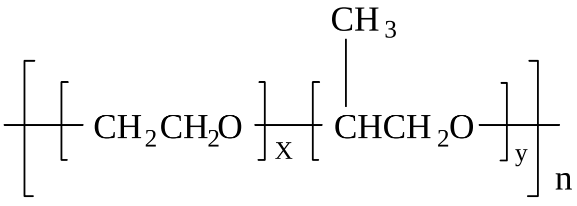

$$\left[\left[CH_2CH_2O \right]_x \left[\overset{CH_3}{\overset{|}{C}}HCH_2O \right]_y \right]_n$$

Poly (ethylene glycol-ran-propylene glycol) (PEPG)

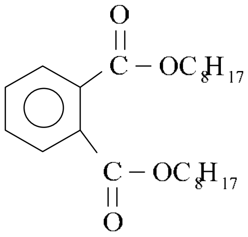

Dioctyl phthalate (DOP)

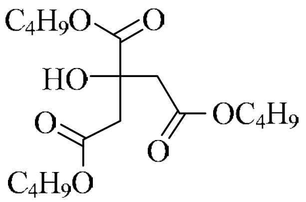

Tributyl citrate (TBC)

$COOH \leftarrow\!\!\!\!(C_nH_{2n})\!\!\!\!\rightarrow COOH$

Acid group n = 4, Adipic acid

n = 8, Sebacic acid

n =10, Dodecanedioic acid

Figure 4.1 Molecular structures of plasticizers

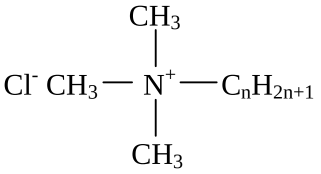

$$Cl^- \; CH_3 - \overset{\displaystyle CH_3}{\underset{\displaystyle CH_3}{N^+}} - C_nH_{2n+1}$$

n= 12-18

Trimethyl tallow quaternary ammonium chloride (M_3T)

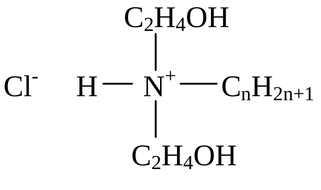

$$Cl^- \quad H - \overset{\displaystyle C_2H_4OH}{\underset{\displaystyle C_2H_4OH}{N^+}} - C_nH_{2n+1}$$

n= 12-18

Tallow bis(2-hydroxyethyl)amine ($HT(OH)_2$)

Figure 4.2 Molecular structure of amine salts

4.2 Organoclay

In this research, the Na-montmorillonite was used as hydrophilic pristine clay. The Na-montmorillonite must be treated with surfactant to convert hydrophilic clays to hydroprobic or organophilic clays.

4.3 Preparation of films by melt processing

4.3.1 Plasticized PLA blown films

PLA pellets was dried in an oven at 60 ^{o}C for 24 h. PLA and plasticizers were compounded into pellets with twin screw extruder (Thermo Hakke Reomix, Germany) attached to rod capillary die, cooling bath and pelletizer. After that, the plasticized PLA pellets were dried in an oven at 60 ^{o}C for 24 h. The mixing ratio between PLA and plasticizer were 97/3, 95/5 and 93/7 w/w which shown in table 4.1. The plasticized PLA blown films were then produced with twin-screw extruder attached to blown film die as shown in table 4.2.

Table 4.1 Operating condition of twin screw extruder for plasticized PLA pellet cutting

Plasticizer content (wt%)	Screw Speed (rpm)	Feeder Speed (rpm)	TS-E1 (^{o}C)	TS-E2 (^{o}C)	TS-E3 (^{o}C)	TS-E4 (^{o}C)	TS-D1 (^{o}C)	TS-D2 (^{o}C)
3	150	80	195	195	195	195	192	192
5	150	80	190	190	190	190	187	187
7	150	80	185	185	185	185	182	182

Table 4.2 Operating condition of twin screw extruder for plasticized PLA blown films

	Neat PLA	PLA+ Acid group			PLA+ PPG			PLA+ DOP			PLA+ TBC			PLA+ PEPG		
		3wt%	5wt%	7wt%	3wt%	5wt%	7wt%	3wt%	5wt%	7wt%	3wt%	5wt%	7wt%	3wt%	5wt%	7wt%
Screw Speed (rpm)	150	150	150	150	150	150	150	150	150	150	150	150	150	150	150	150
Feeder Speed	80	80	80	80	80	80	80	80	80	80	80	80	80	80	80	80
Roll Speed	380	380	380	380	380	380	380	380	380	380	380	380	380	380	380	380
Torque (n.m)	60	55	55	60	50	50	45	45	50	50	60	55	50	45	45	40
TS-E1	185	165	160	153	185	180	175	180	175	170	180	175	172	177	173	163
TS-E2	185	165	160	153	185	180	175	180	175	170	180	175	172	177	173	163
TS-E3	185	165	160	153	185	180	175	180	175	170	180	175	172	177	173	163
TS-E4	185	165	160	153	185	180	175	180	175	170	180	175	172	177	173	163
TS-D1	182	162	157	150	182	177	172	177	172	167	177	172	169	174	170	160
TS-D2	182	162	157	150	182	177	172	177	172	167	177	172	169	174	170	160

4.3.2 PLA/clay nanocomposite blown films

After the suitable plasticizer was obtained to produce, the plasticized PLA films, it was mixed with organoclay at 1, 3 and 5 wt% as the method used in preparing the plasticized PLA blown films. Temperature in process was showed in table 4.3 and 4.4.

Table 4.3 Operating condition of twin screw extruder for PLA/clay pellet cutting

Organoclay loading (wt%)	Screw Speed (rpm)	Feeder Speed (rpm)	TS-E1 (^oC)	TS-E2 (^oC)	TS-E3 (^oC)	TS-E4 (^oC)	TS-D1 (^oC)	TS-D2 (^oC)
1	150	80	185	185	185	185	182	182
3	150	80	180	180	180	180	177	177
5	150	80	180	180	180	180	177	177

Table 4.4 Operating condition of twin screw extruder for PLA/clay blown films

	PLA+ PPG(5wt%) + $HT(OH)_2$			PLA+ PPG(5wt%) + M_3T		
	1wt%	**3wt%**	**5wt%**	**1wt%**	**3wt%**	**5wt%**
Screw Speed (rpm)	150	150	150	150	150	150
Feeder Speed	80	80	80	80	80	80
Roll Speed	380	380	380	380	380	380
Torque (n.m)	50	45	40	50	40	35
TS-E1	170	167	162	168	165	162
TS-E2	170	167	162	168	165	162
TS-E3	170	167	162	168	165	162
TS-E4	170	167	162	168	165	162
TS-D1	167	164	159	165	162	159
TS-D2	167	164	159	165	162	159

4.4 Characterizations

4.4.1 Differential scanning calorimetery (DSC)

Differential scanning calorimetery (DSC) measurements were performed by using a differential scanning calorimeter (TA Instruments 2910). All of the blown films (5-10 mg) were tested at a heating rate of 10 ^{o}C/ min in nitrogen atmosphere from 30 to 200 ^{o}C. The percent of crystallinity of all the blown films were estimated as equation 1 according to the enthalpy obtained from the DSC curves.

$$X_c = \frac{(\Delta H_m - \Delta H_c)}{(\Delta H_o \, x \, \Phi)} x100 \qquad (1)$$

where ΔH_m and ΔH_c are the enthalpies of the melting and cold crystallization of mixing PLA, and ΔH_o (93 J/g) is the melting enthalpy of 100% crystalline PLA [6]. A parameter Φ, the weight fraction of the matrix, is introduced to eliminate the weight contribution of plasticizer [15].

4.4.2 Mechanical testing

In this study, tensile testing of the blown films was performed according to ASTM D 882 by using Universal Testing Machine (Instron 5567, NY, USA), which was used to determine tensile strength, Young's modulus and elongation at break. All tested specimens were cut to rectangular shape with the width of 10 mm and the length of 100 mm. The used crosshead speed for this tensile testing is 12.5 mm/min with a 1 kN load cell.

4.4.3 X-ray diffraction (XRD)

The structure of the nanoclay and the PLA composite films were evaluated with XRD measurements. XRD was performed on a D8 advance diffractometer (BRUKER German) with CuK_α radiation of wavelength 1.542 Å. The voltage and current used in this analysis were 40kV and 30 mA, respectively. The interlayer spacing of the layer silicate was calculated using the Bragg's equation that is shown in equation 2.

$$2d\sin\theta = n\lambda \qquad (2)$$

Where

λ = The wavelength of the X-ray radiation used in the diffraction experiment which is 1.542 Å

d = The spacing between diffractional lattice planes

θ = The measured diffraction angle

n = Peaks corresponding to the basal reflection [5] or n=1

4.4.4 Dynamic mechanical analysis (DMA)

Dynamic mechanical properties of neat PLA and the modified PLA blown films were performed in a tension mode by DMA equipment (NETZSCH, DMA 242). The tested specimens had a width of 10 mm, length of 30 mm and thickness 0.035 mm. Storage modulus, loss modulus and tan δ were recorded at a heating rate of 2^{o}C/min. The frequency was set at 1.0 Hz. All measurements were carried out under inert N_2 atmosphere.

4.4.5 Ultraviolet-visible spectrometer (UV-vis)

Optical properties of modified PLA blown films were determined by measuring the percent transmittance at 660 nm [18] using a UV-vis spectrophotometer (Model Lambda 650, Perkin Elmer Co., USA). The tested films had a width of 20 mm, length of 20 mm and thickness 0.035 mm.

4.4.6 Gas barrier testing

Oxygen permeation (OTR) and water vapor permeation (WVTR) of PLA/clay nanocomposite blown films and neat PLA blown films were carried out in accordance with ASTM standards D3985 and E96, respectively. Oxygen permeation was measured using a MOCON OX-TRAN model 2/21 with an oxygen flow rate of 40 cm^3/min at 0 % relative humidity and 23 ^oC. All of blown film sample for OTR test were required in circular shape with diameter 100 cm^2 and thickness 0.035 mm. Water vapor permeation was measured using a MOCON PERMATRAN-W model 398 with nitrogen flow rate of 250 cm^3/min at 90 % relative humidity and 37.8 ^oC. All of blown film sample for WVTR test were required in circular shape with diameter 50 cm^2 and thickness 0.035 mm. Oxygen and water vapor permeation were carried out at atmospheric pressure.

CHAPTER V

RESULTS AND DISCUSSION

The experimental results from various tests on the modified PLA blown films will be demonstrated and discussed in this chapter which is divided into 3 parts. The first part concentrates on studying the effect of types and loading of plasticizer on properties of plasticized PLA blown films. The second part focuses on the effect of the molecular weight of plasticizer on properties of plasticized PLA blown films. Then the effect of surfactant types and organoclay loading on properties of PLA/clay nanocomposite blown films is proposed in final part.

5.1 Effect of plasticizer types and loading on properties of plasticized PLA blown films

Chemical structure and loading of plasticizers affect the thermal, thermomechanical and mechanical properties of plasticized PLA blown films. The plasticizers used in this study include polypropylene glycol (PPG) whose molecular weight is 1200 g/mol representing by PPG(1200), poly (ethylene glycol-co-propylene glycol) (PEPG), dioctyl phthalate (DOP), tributyl citrate (TBC) and adipic acid.

The plasticized PLA blown films were prepared by twin screw extruder attached to blow films die at screw speed of 150 rpm and processing temperature in the barrel was set at 155-195 ^{o}C and die’s temperature was set at 150-190 ^{o}C.

5.1.1 Thermal properties

The thermal properties of all samples were determined by differential scanning calorimetry (DSC) which shows three characteristic transitions, i.e, glass transition temperature (T_g), cold crystallization temperature (T_{cc}) (exothermic peak) and melting temperature (T_m) (endothermic peak). All the thermal properties of plasticized PLA blown films were summarized in Appendix A.

Figure 5.1 shows the DSC thermograms of neat PLA and PLA blown films containing 3 wt% of plasticizer. Addition of the plasticizers decreased T_g and T_{cc} because plasticizers penetrate into polymer matrix increasing the polymer chain movement [4]. Furthermore, it was found that different chemical structure of plasticizers cause the enthalpy of T_{cc} and T_m increased which can be determined by the area under cold crystallization and melting peaks. Moreover, PLA films containing adipic acid gave the highest enthalpy, which indicated the highest degree of crystallinity, compared to that with other plasticizers because flexibility, hydroxyl group and symmetry of adipic acid’s backbone cause polymer’s chain attachment forming a crystal [6]. The T_m of plasticized PLA blown films slightly decreased from 153 ^oC to 150 ^oC at 3 wt% of plasticizer. Moreover, adding different types of plasticizer in PLA did not significantly affect the T_m of plasticized PLA films. Furthermore, the degree of crystallinity of plasticized PLA blown films was higher than that of neat PLA blown film, which is shown in table A.1 (Appendix A). This result can be explained that plasticizers induce heterogeneous crystallization [3-6].

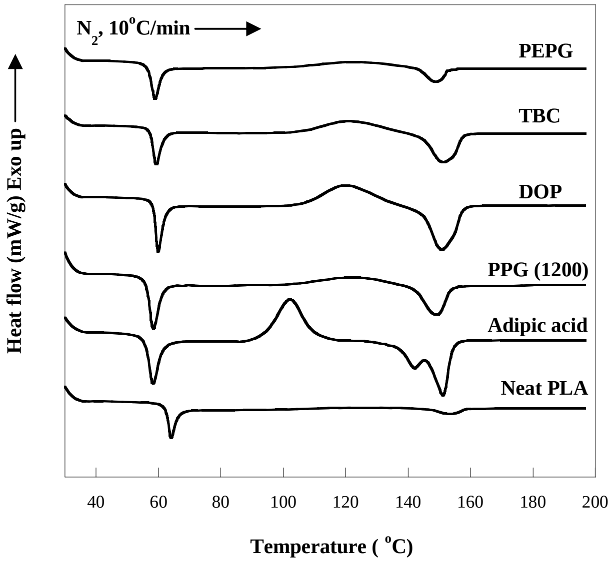

Figure 5.1 DSC thermograms recorded at a heating rate of 10 °C/min under N_2 for neat PLA and PLA blown films containing 3 wt% of plasticizer

Figure 5.2 displays the DSC graphs of neat PLA and PLA blown films containing 3, 5 and 7 wt% polypropylene glycol, PPG(1200). The addition of PPG(1200) decreases T_g of PLA from 63 °C to 57 °C, 53 °C and 50 °C by adding 3, 5, and 7 wt% PPG(1200), respectively. Furthermore, T_{cc} decreases when PPG(1200) is added. Especially, at 7 wt% PLA/PPG(1200) blown film, T_{cc} of PLA dramatically decreases from 124 °C to 105 °C. The incorporation of plasticizer increases the degree of crystallinity of PLA resulting from plasticizer acts like nucleating agent which affects PLA chain attachment forming crystal such as α', α, β and γ [26-28]. The α form of PLA originates from the arrangement and packing of molecular chains in the crystalline phase because of high chain's interactions of hydrogen bonding. The α' phase is formed at lower temperature than the α phase. The molecular packing within the unit cell of α' form PLA is looser and disordered, corresponding to weaker chain's interaction [26]. The β phase is mostly prepared by hot-drawing the melt

PLA or stretching the α form at high temperature and high draw ratio (DR). The γ form has been obtained via epitaxial crystallization on hexamethylbenzene (HMB) substrate [27]. The T_m of plasticized PLA blown films slightly changes with an increased of plasticizer's content. Furthermore, 3 wt% PLA/PPG(1200) film exhibits single melting peaks of T_m but 5 and 7 wt% PLA/PPG(1200) film reveal multiple melting peaks because PPG's content over 3 wt% affect extremely decreases T_c causing the reorganization of crystal structure. Including, the reorganization of crystalline phase composed of α' form appears at low T_c about 110 ^oC (low thermodynamic stability, T_m 148 ^oC) and α form appears at high T_c about 125 ^oC (high thermodynamic stability, T_m 153 ^oC). In case of blown films of plasticized PLA at 7 wt% shows the bleeding of plasticizer after 1 month which implies the phase separation between plasticizer and PLA [3, 4]. The thermal behavior of other plasticized PLA blown films obtained from DSC demonstrates similar results as mentioned above.

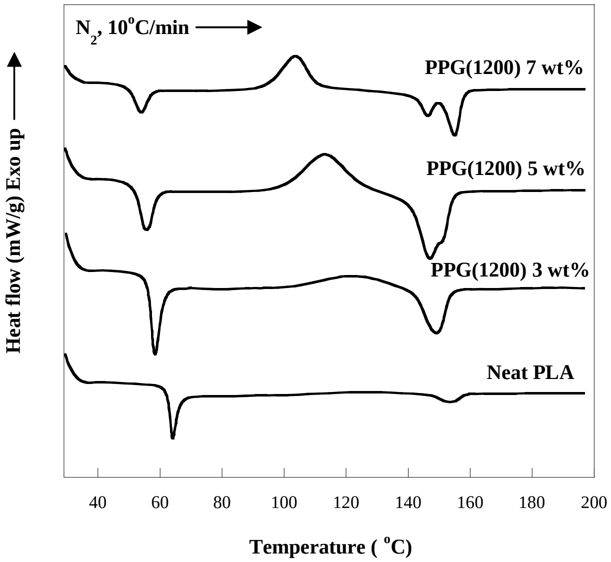

Figure 5.2 DSC thermograms recorded at a heating rate of 10 ^oC/min under N_2 for neat PLA and PLA blown films containing 3, 5 and 7 wt% PPG(1200)

5.1.2 Thermomechanical properties

Dynamic mechanical analysis (DMA) is employed to measure the dynamic response of the plasticized PLA blown films under a given set of conditions. The analysis of the storage modulus, loss modulus and tan δ curves is very useful to investigate the performance of the blown films under stress and temperature. All the thermomechanical properties of plasticized PLA blown films are summarized in table B.1 (Appendix B).

Figure 5.3 a) and b) show the storage modulus and tanδ, respectively, as a function of temperature for blown films of neat PLA and PLA containing 3 wt% of plasticizer. All plasticized PLA blown films exhibit slightly lower storage modulus at glassy state and tanδ peak than those of neat PLA because all plasticizer cause chain's relaxation in part of amorphous phase [4]. In Figure 5.3 a) the storage modulus is stable at low temperature, which is glassy state, then it rapidly decreases during transition state in which this region is concerned with T_g, and the final region is rubbery plateau [13]. The plasticizers decrease the storage modulus at glassy state of neat PLA from 2800 MPa to about 2200 MPa and T_g from 76 ^oC to 68 ^oC but they increase the storage modulus at rubbery plateau of neat PLA from 4 MPa to 7-19 MPa. Moreover, storage modulus at rubbery plateau of PLA added adipic acid is higher than other plasticizers because adipic acid gave the highest degree of crystallinity which is shown in DSC results. In Figure 5.3 b), the temperature of tan δ peak is identified as T_g which shifted to lower temperature from 80 ^oC to about 73 ^oC. The T_g obtained tan δ peak is few degrees higher than that determined from DSC because 1 Hz of DMA data may correspond to heating rate of DSC in the range 20-40 ^oC/min [5, 13].

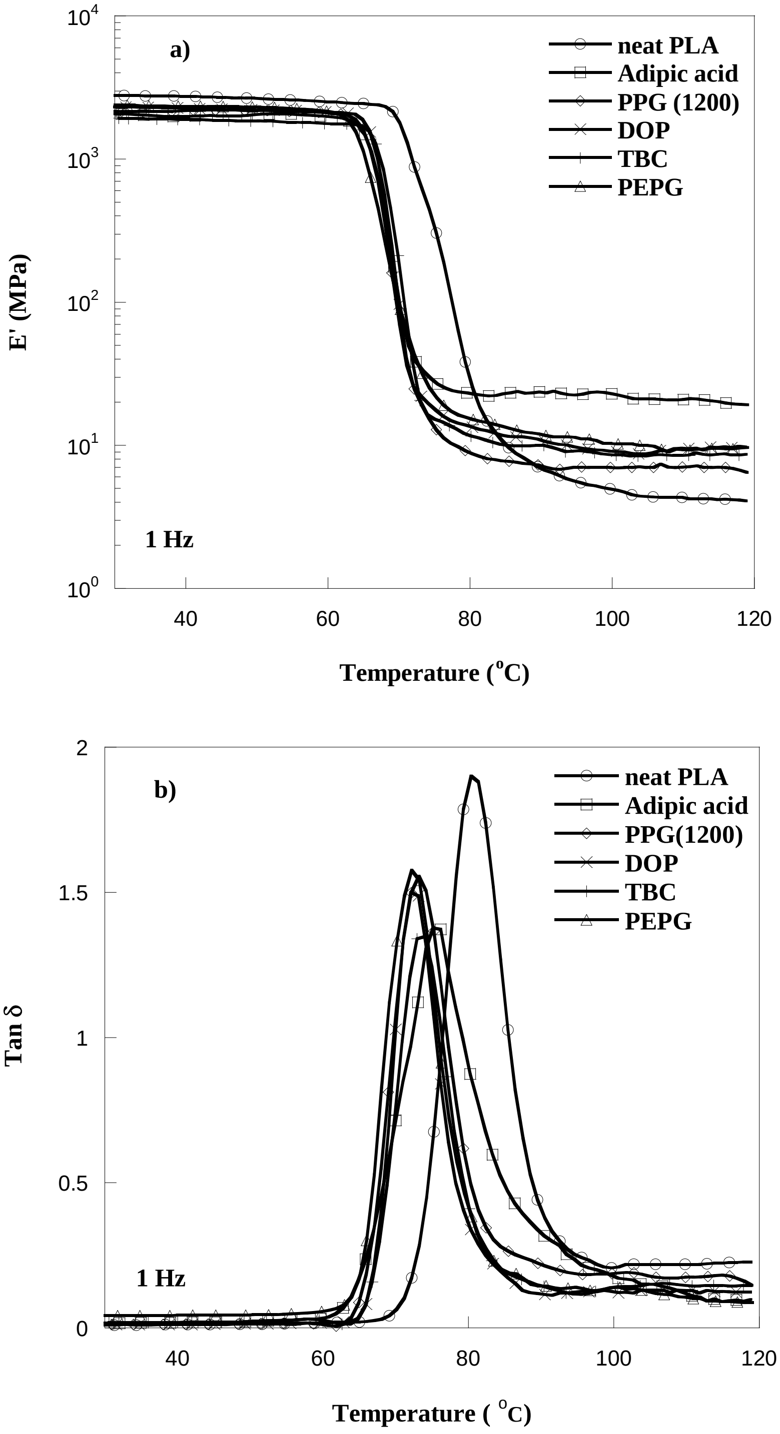

Figure 5.3 Temperature dependence of (a) the storage modulus (E') and (b) tan δ for neat PLA and PLA blown films containing 3 wt% of plasticizer

Figure 5.4 a) and b) show the storage modulus and tan δ of neat PLA and PLA blown films containing 3, 5 and 7 wt% PPG(1200). The storage modulus at glassy state decreases from 2800 MPa to 2166, 2010 and 1832 MPa at PPG(1200) content of 3, 5 and 7 wt%, respectively but the storage modulus at rubbery plateau tended to increase. Furthermore, storage modulus at rubbery plateau of PLA added PPG(1200) at 7 wt% extremely increases because PPG(1200) extremely decreases T_c at 7 wt%, which is shown in DSC results. In Figure 5.4 b) tan δ peak decreases from 80 ^{o}C to 73, 69 and 66 ^{o}C, at PPG(1200) content of 3, 5 and 7 wt%, respectively. Furthermore, the height of tan δ peak of neat PLA is highest due to no restriction the chain's motion which it identifies amorphous polymer. The plasticized PLA film shows lower tan δ peak than neat PLA film because the crystalline region restricts motion of chain which it identifies semicrystalline polymer. The decrease in tan δ height is associated with motion of polymer's chains which are hindered. This result indicates that the content of PPG(1200) affects expansion of PLA chains [13].

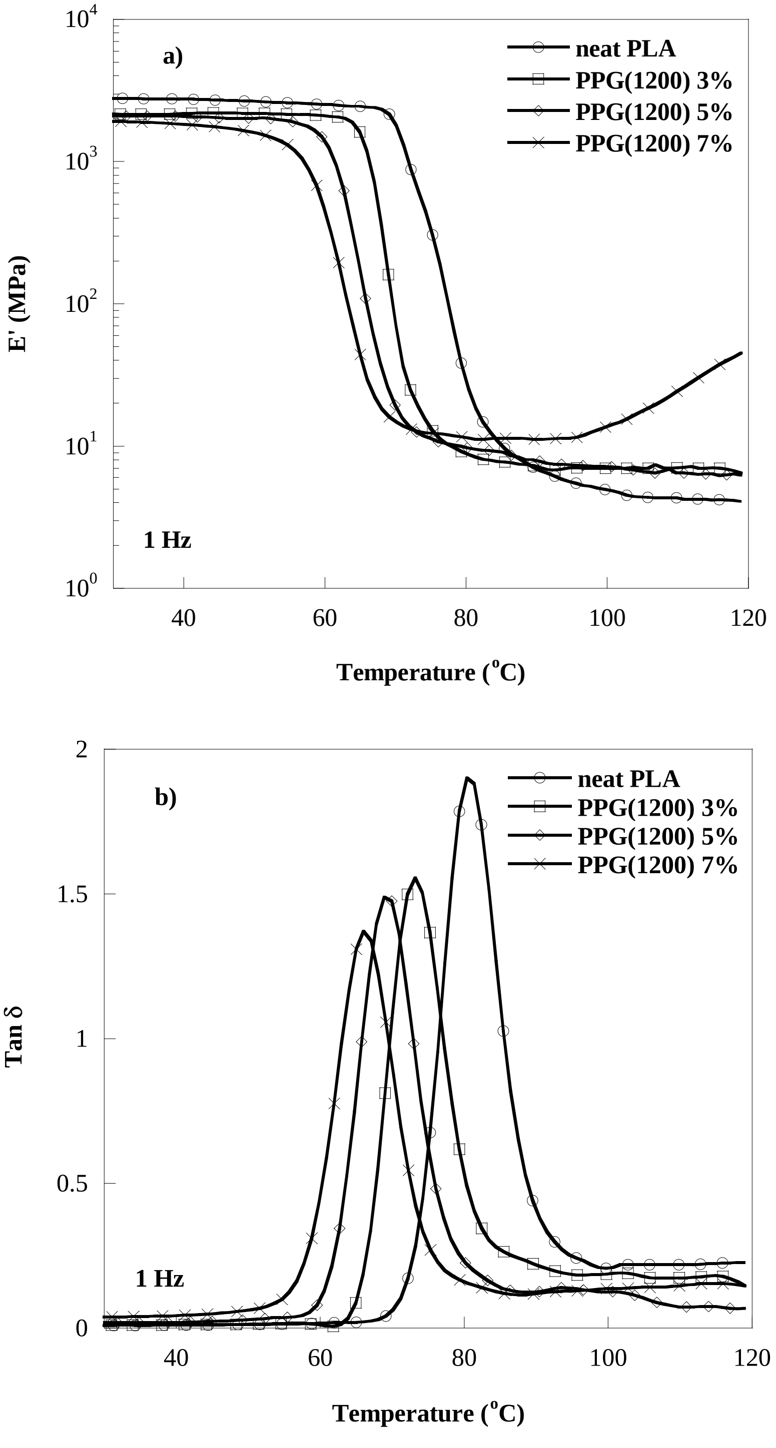

Figure 5.4 Temperature dependence of a) the storage modulus (E') and b) tan δ for neat PLA and PLA blown films containing 3, 5 and 7 wt% polypropylene glycol, PPG(1200)

5.1.3 Mechanical properties

The tensile test was used to determine the mechanical properties, such as tensile strength, tensile modulus and elongation at break of blown films according to ASTM D882 by universal testing machine (Instron 5567). The tensile strength of material was defined as the maximum tensile stress which material began to deform. The tensile modulus was determined by the first linear slope of stress-strain curve which was used to indicate the stiffness of material. The elongation at break was defined as strain at maximum tensile strain at break or at the rupture of the specimen. All the mechanical properties of plasticized PLA blown films are summarized in Appendix C.

From Figure 5.5 neat PLA, as a kind of stiff and brittle polymer which displays no yield point, shows 3.3% of elongation at break in machinery direction (MD) and 58 MPa of the tensile strength. On the contrary, mixing PLA with plasticizer shows distinct yield point and stable neck growth through cold drawing. The stress-strain curves indicated that the fracture behavior of the specimen displayed a transition from brittle fracture to ductile fracture [3]. The elongation at break of mixing PLA with 3 wt% of PPG(1200) increased from 3.3% (neat PLA) to 23%; whereas the tensile strength is 8 MPa lower than that of neat PLA. This result indicated that plasticizers affect on structure of PLA. The mechanical properties in transverse direction (TD) show similar result in neat PLA and plasticized PLA blown films but these values are less than those in MD because in process of blown film the TD line only depends on flow rate of air but the MD line depends on flow rate of air and pull rate of nip roll, which affect the organization of PLA’s molecular chain.

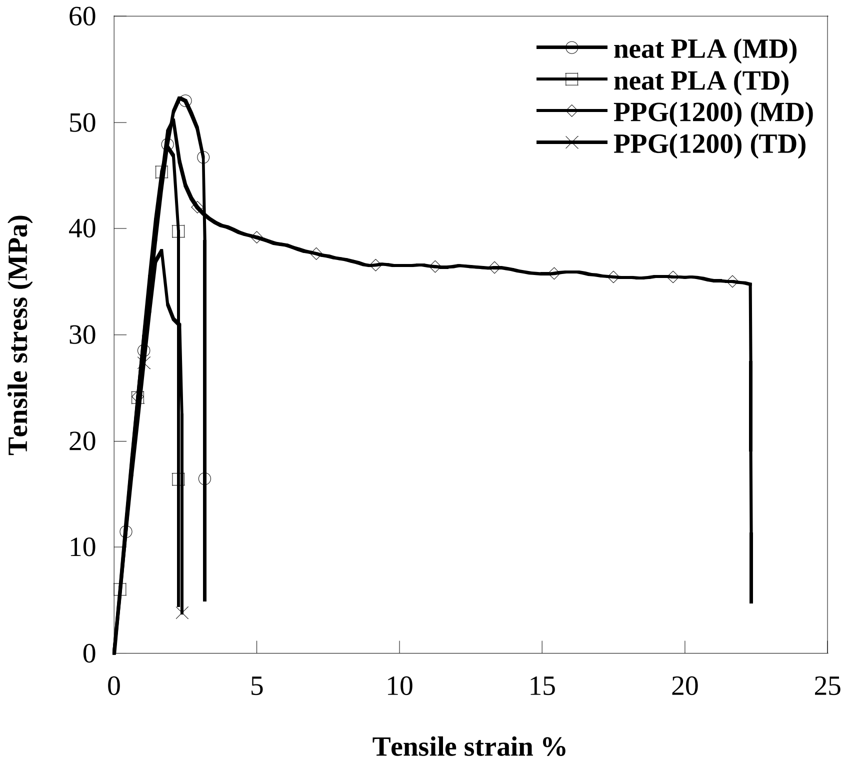

Figure 5.5 Stress-strain curves of the neat PLA and PLA blown films containing 3 wt% polypropylene glycol, PPG(1200) in machinery direction (MD) and transverse direction (TD)

Tensile strength and tensile modulus of blown films in MD are illustrated in Figure 5.6 a) and b), respectively. Adding plasticizer into PLA matrix can decrease rigidity and increase ductility of PLA films. Therefore, the addition of plasticizer causes the decrease of tensile strength and tensile modulus because plasticizer penetrates between the polymer chains and decreases the intermolecular forces which lowers polymer chain’s cohesion [15].

The tensile strength and tensile modulus of neat PLA film are 58 and 2886 MPa, respectively. Tensile strength and tensile modulus of PLA plasticized with 7 wt% PPG(1200) decreases to be 37 and 2115 MPa, respectively. Thus PPG strongly affects the tensile strength and tensile modulus of the blown films. In addition, it was also found that PLA added with 7 wt% of adipic acid shows the increase in tensile strength and tensile modulus because molecular attraction between molecule of polymer and adipic acid increased in which it extremely increased degree of crystallinity of neat PLA about 20 times as evidenced by DSC result.

The elongation at break of neat PLA is 3.3% as shown in Figure 5.6 c) which is found that PLA added with PPG(1200) exhibits the highest elongation at break. However, low contents of plasticizer hardly affect the elongation at break of PLA, i.e., PLA containing 3 wt% of plasticizer. The increase of PPG(1200) content to 5 wt% increases the elongation at break to about 110%. Moreover, the elongation at break reached 150% for the 7 wt% of PPG(1200) content in which an increase of elongation at break results from the PPG(1200) comprising a poly(alkylene ether) segments, longer chain (higher molecular weight) than other plasticizers. Furthermore, other plasticizers have functional group such as aromatic ring, branch and carboxylic acid which obtruct mobility of polymer's chain [29]. The plasticizers increase the ability of PLA to be plastic deformed which is reflected in the increase of elongation at break. However, blown films of plasticized PLA at 7 wt% shows the bleeding of plasticizer after 1-month storage. Therefore, the optimal plasticizer content for this study is 5 wt%.

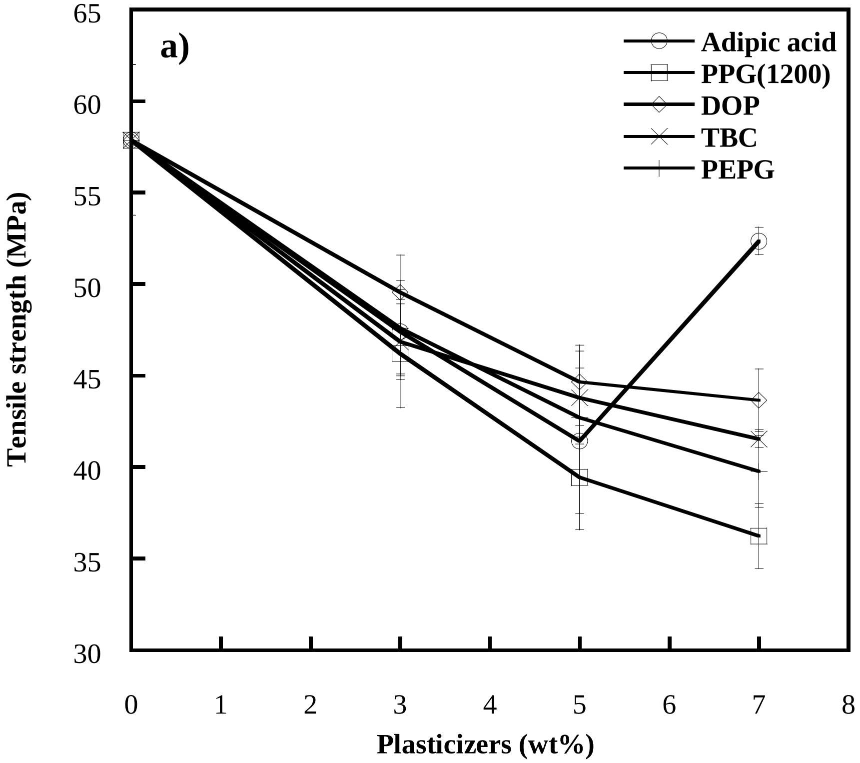
a)
Adipic acid
PPG(1200)
DOP
TBC
PEPG
Tensile strength (MPa)
65
60
55
50
45
40
35
30
0
1
2
3
4
5
6
7
8
Plasticizers (wt%)

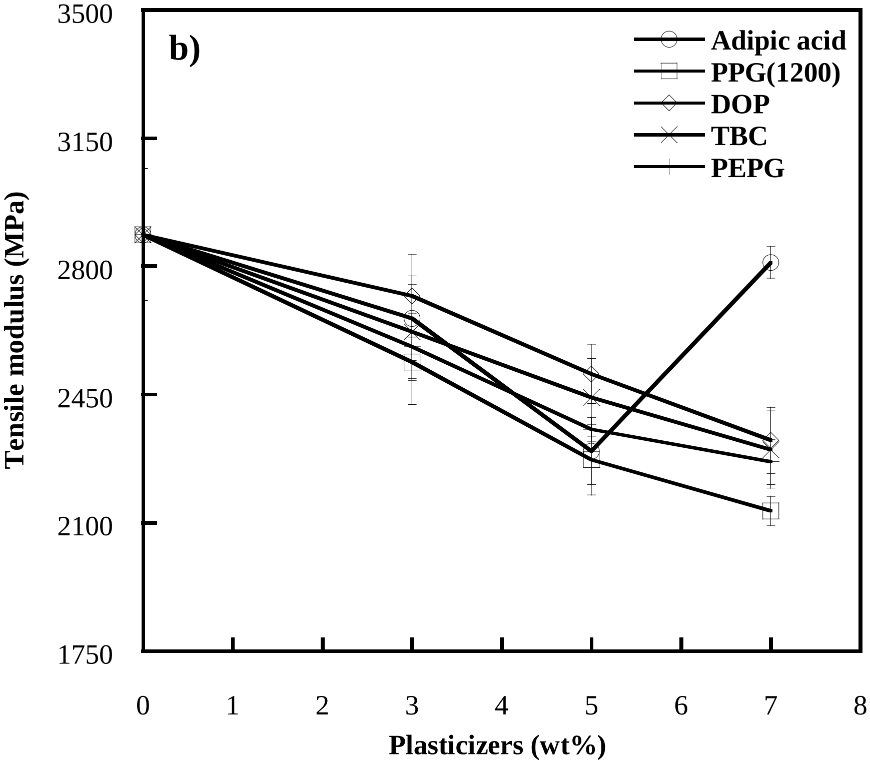
b)
Adipic acid
PPG(1200)
DOP
TBC
PEPG
Tensile modulus (MPa)
3500
3150
2800
2450
2100
1750
0
1
2
3
4
5
6
7
8
Plasticizers (wt%)

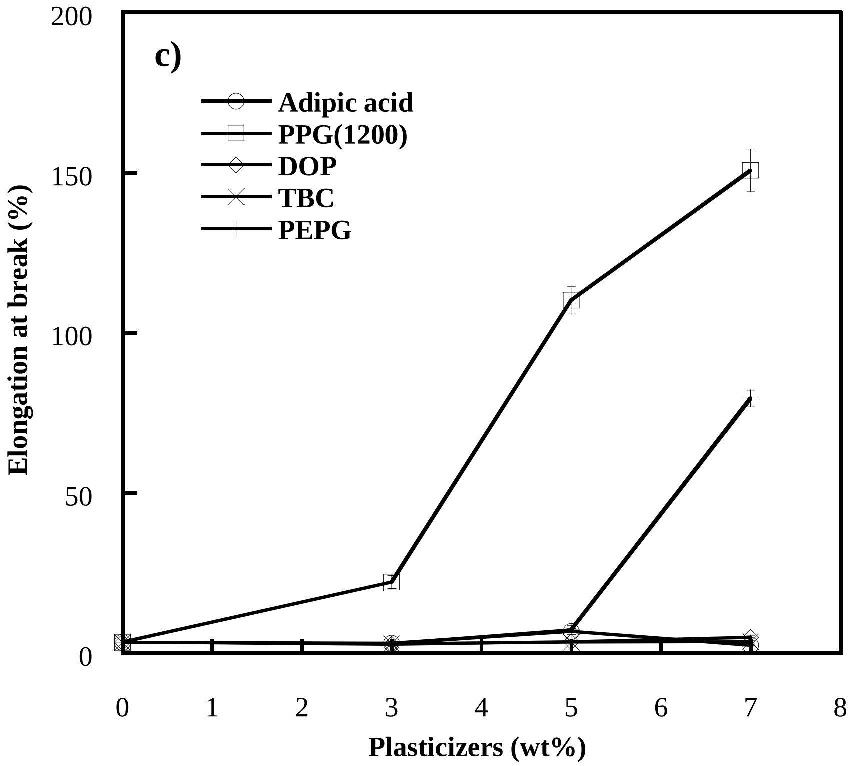

Figure 5.6 mechanical properties of neat PLA and PLA blown films containing 3, 5, and 7 wt% plasticizers a) tensile strength b) tensile modulus c) elongation at break

5.2 Effect of the molecular weight of PPG plasticizer on properties of plasticized PLA blown films

In section 5.1, the chemical structure and loading of plasticizers on properties of plasticized PLA blown films were studied. In this section, the effect of molecular weight of plasticizer on properties of plasticized PLA blown films was also investigated. The plasticizers were used in this study including polypropylene glycol (PPG) having molecular weight (MW) of 1200 and 2000 g/mol, representing by PPG(1200) and PPG(2000).

5.2.1 Thermal properties

Figure 5.7 shows DSC thermogram comparing neat PLA blown film with PLA containing 3, 5 and 7 wt% of PPG(1200) and PPG(2000). The peaks on DSC thermogram displayed glass transition, cold crystallization and melting peaks. From DSC graph, the T_g and T_{cc} of PLA containing PPG(1200) and PPG(2000) occur at lower temperature than those of neat PLA. The lowest T_g was clearly observed for the PPG having the low MW, PPG(1200). The MW of PPG causes the area under of the cold crystallization and melting peaks increased which increases the degree of crystallinity, although the difference are quite small which is about 1-2 %. This result indicated that MW of plasticizer affects T_g but does not affect on the degree of crystallinity because high MW plasticizer penetrate between polymer chain’s more difficult than shorter chain plasticizer [14]. Furthermore, the PLA mixing with all of wt% of PPG(2000) and PLA mixing with over 3 wt% of PPG(1200) exhibit two melting peaks implying two different crystal structures [3, 4]. All data of thermal properties of plasticized PLA blown films are shown in table A.2 (Appendix A).

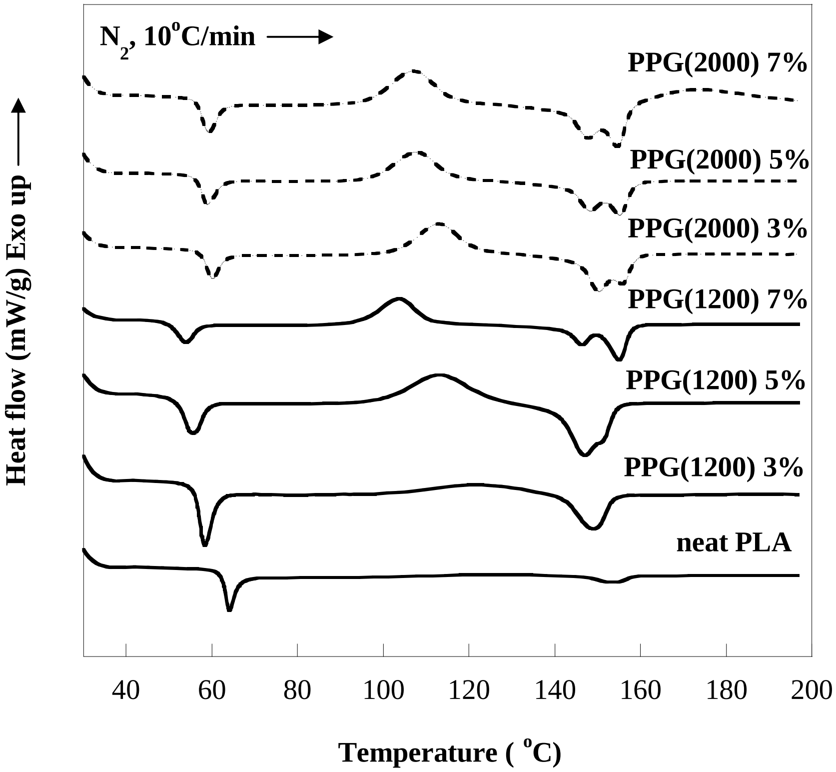

Figure 5.7 DSC thermograms recorded at a heating rate of 10 ^{o}C/min under N_2 for neat PLA and PLA blown films containing 3, 5 and 7 wt% PPG(1200) and PPG(2000)

5.2.2 Thermomechanical properties

Figure 5.8 a) and b) show the storage modulus and tanδ respectively, as a function of the temperature of blown films of neat PLA and PLA containing 3 wt% PPG(1200) and PPG(2000). The storage modulus at glassy state of neat PLA, which is considered at 30 ^{o}C, is 2800 MPa. When both kinds of PPG was added, the storage modulus at glassy state decreases to 2190-2200 MPa and it was found that PPG decreases T_g from 80 ^{o}C to 73-75 ^{o}C and it decreases height of tan δ peak of neat PLA which it identifies semicrystalline polymer. T_g of PLA containing PPG(1200) is lower than that of PLA containing PPG(2000) because low MW PPG can enhance mobility of PLA chains better than high MW PPG [3]. The data of thermomechanical properties are concluded in table B.2 (Appendix B).

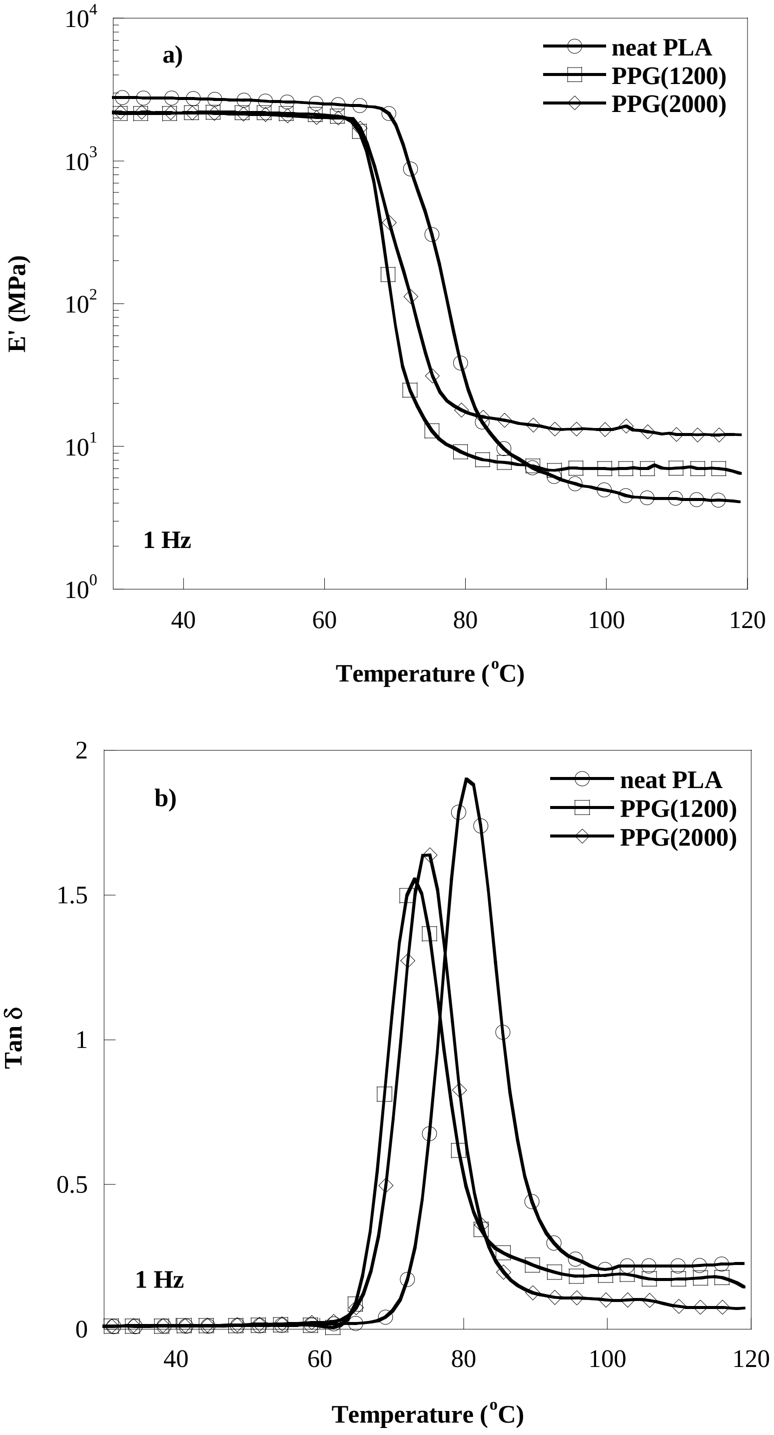

Figure 5.8 Temperature dependence of a) the storage modulus (E') and b) tan δ for neat PLA and PLA blown films containing 3 wt% PPG(1200) and PPG(2000)

5.2.3 Mechanical properties

Figure 5.9 a) and b) demonstrate the tensile strength and tensile modulus of neat PLA and PLA blown films containing 3, 5, and 7 wt% PPG(1200) and PPG(2000), respectively. Addition of PPG leads to decrease of tensile strength and tensile modulus of PLA due to lower molecular chain's attraction, and it was also found that high MW plasticizer induces more expansion of polymer chain than low MW one resulting in decrease in intermolecular force in polymer chains [15]. The PLA mixing with 3, 5 and 7 wt% of PPG(1200) and PPG(2000) causes the tensile strength and tensile modulus of neat PLA decrease from 58 to 46-30 MPa and from 2886 to 2540-2040 MPa, respectively.

The elongation at break increases when the PPG content increases, and the effect of MW of PPG on film's flexibility is shown in Figure 5.9 c) where the elongation at break is apparently increased with increasing PPG content. However, it is also found that elongation at break of film containing low MW plasticizer is higher than that with high MW plasticizer because it penetrates into polymer matrix easier than the low MW one [15]. The elongation at break extremely increases from 3.3% to 150% with PLA containing 7 wt% PPG(1200). The data of mechanical properties are concluded in Appendix C.

Furthermore, study on the number of carbon atom in backbone of acid-type plasticizer including adipic acid, sebacic acid and dodecanedioic acid, reveals that properties of plasticized PLA did not depend on the number of carbon atom in backbone of plasticizers as shown in table A.3, B.3 and Appendix C.

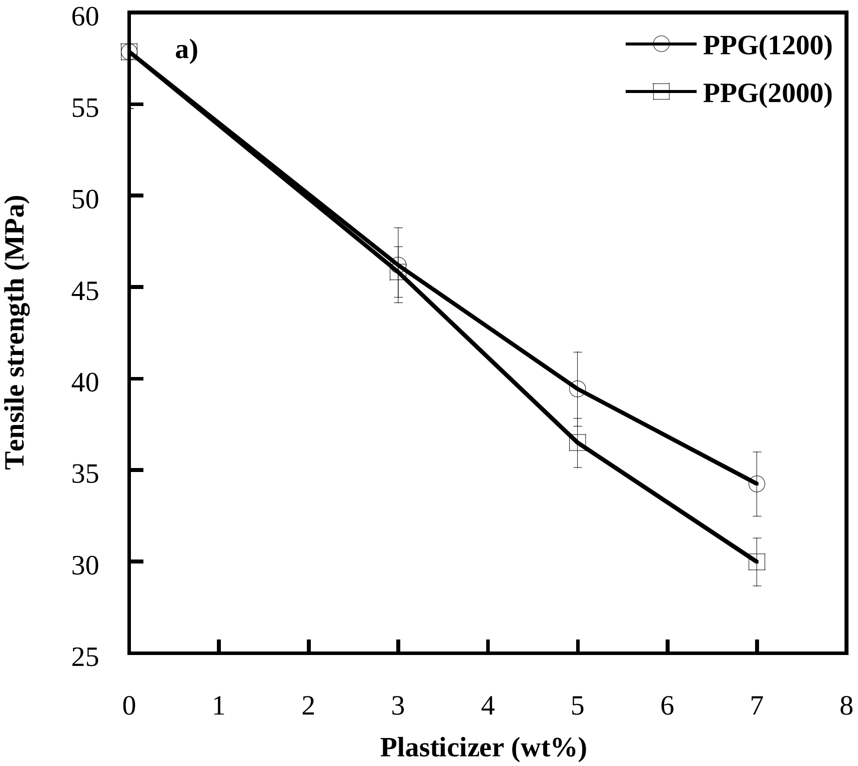
a)
PPG(1200)
PPG(2000)
Tensile strength (MPa)
60
55
50
45
40
35
30
25
0
1
2
3
4
5
6
7
8
Plasticizer (wt%)

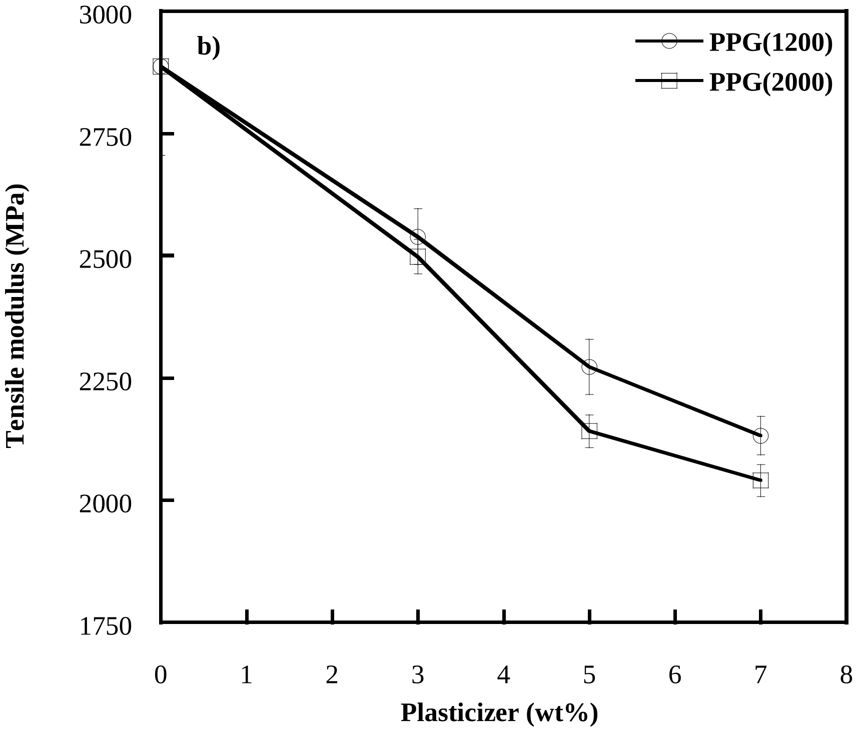
b)
PPG(1200)
PPG(2000)
Tensile modulus (MPa)
3000
2750
2500
2250
2000
1750
0
1
2
3
4
5
6
7
8
Plasticizer (wt%)

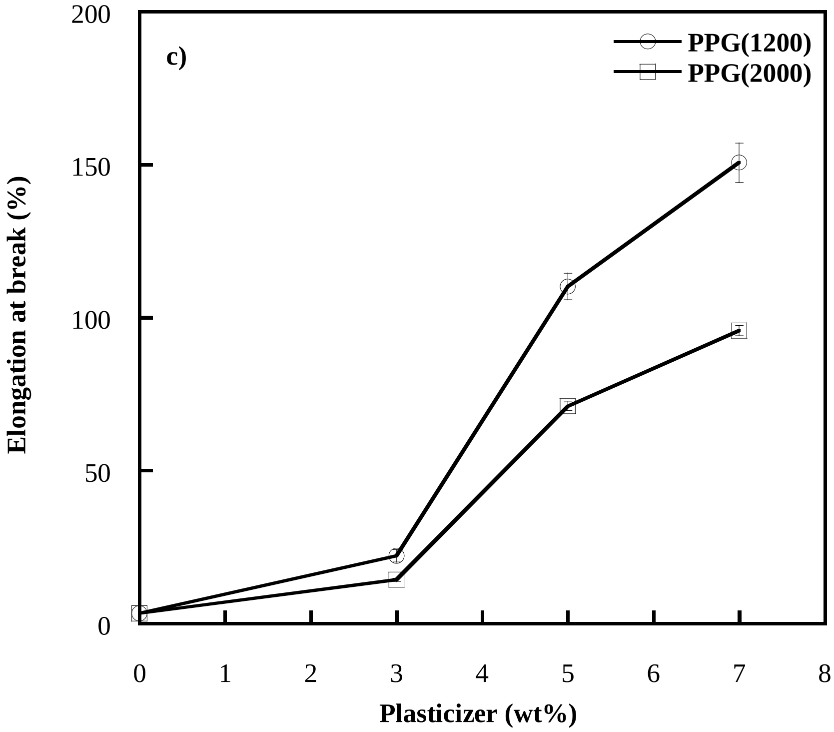

Figure 5.9 Mechanical properties of neat PLA and PLA blown films containing 3, 5, and 7 wt% PPG(1200) and PPG(2000) a) tensile strength b) tensile modulus c) elongation at break

5.3 Effect of surfactant types and organoclay loading on properties of PLA/clay nanocomposite blown films

Although adding plasticizer increases elongation at break of film but tensile strength and tensile modulus of film decrease. Therefore, adding nanoclay treated with surfactant would improve tensile strength and tensile modulus of PLA film. However, clay is incompatible with PLA during blown film process leading to agglomeration of clay. Thus, surfactant will be used to increase dispersion of clay and compatibility between PLA and clay. It was found from previous chapter that by adding 5 wt% of PPG(1200) into PLA optimal properties of PLA blown film would be obtained. In this part the effect of surfactant on clay's dispersion and properties of PLA containing 5 wt% PPG(1200) will be studied. The hydrophilic surface layers of Na-montmorillonite were modified by dispersing Na-montmorillonite uniformly into organic modifier solution, also known as surfactant. The surfactant types were investigated because the structure and reaction affected the interlayer spacing of clay which leads to enhanced properties, espectially in term of mechanical, thermal and gas barrier properties. Furthermore, the surfactant also acts as compatibilizer giving better compatibility between polymer and clay. The surfactants were used in this study including trimethyl tallow quaternary ammonium chloride, represented by M_3T, and tallow bis(2-hydroxyethyl) amine, represented by $HT(OH)_2$.

5.3.1 Degree of clay dispersion

The interlayer spacing of pristine clay, organoclay and the degree of clay dispersion of PLA/clay nanocomposites were evaluated with X-ray diffraction in which the interlayer spacing was calculated using the Bragg's equation. Interlayer spacing and the diffraction peaks of pristine clay, organoclay and nanocomposite films were summarized in table D.1 (Appendix D).

X-ray diffraction pattern of the pristine clay (MMT) and two different types of organoclay are shown in Figure 5.10. The XRD pattern of MMT reveals the diffraction peaks at $2\theta = 7.03^{o}$ corresponding to an interlayer spacing of 1.25 nm. MMT modified by $HT(OH)_2$) displayed the diffraction peaks at $2\theta = 4.47^{o}$ and 6.78^{o} corresponding to an interlayer spacing of 1.97 and 1.30 nm, respectively. In addition, MMT modified by M_3T displayed the diffraction peaks at $2\theta = 2.17^{o}$, 4.69^{o} and 6.67^{o} corresponding to an interlayer spacing of 4.06, 1.89 and 1.32 nm, respectively. Besides, the interlayer spacing of organoclay at 4.06, 1.89 and 1.32 nm corresponds to orientation of surfactant's chain in clay layer form paraffin, bilayer and monolayer structure, respectively [9, 30]. The higher interlayer spacing of organoclays, as compared to the pristine clay, is due to the penetration of surfactant's chain between the clay layer [20]. Furthermore, it is also found that incorporating M_3T into clay had more interlayer spacing than incorporating $HT(OH)_2$ because the hydroxyl group of surfactant restricts stretching of long alkyl chain (C_nH_{2n+1}) [30].

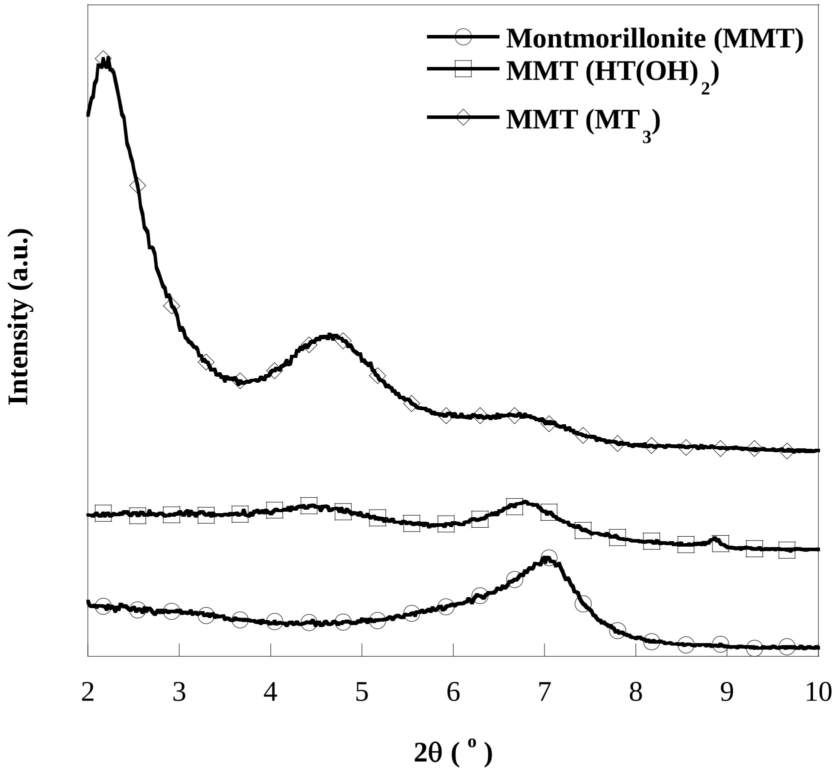

Figure 5.10 X-ray diffraction patterns of pristine clay (MMT) and of organoclays modified by M_3T and $HT(OH)_2$

The clay treated with $HT(OH)_2$, represented by $MMT/HT(OH)_2$, and that with M_3T, represented by MMT/M_3T, are melt-mixed with plasticized PLA by twin screw extruder attached to blown film die at 1, 3 and 5 wt% of $MMT/HT(OH)_2$ and MMT/M_3T. They are called PLA/clay nanocomposite films whose XRD patterns were shown in Figure 5.11 a) and b), respectively. From Figure 5.11 a), the diffraction peak of films containing 1, 3 and 5 wt% $MMT/HT(OH)_2$ is observed at $2\theta = 5.30^{o}$, 4.58^{o} and 4.78^{o} corresponding to an interlayer spacing of 1.66, 1.92 and 1.84 nm, respectively which it indicated that increasing organoclay loading affects an interlayer spacing increased because MMT/HT(OH)$_2$ has hydroxyl group in which PLA's chain can insert between clay layer causing intercalated nanocomposite. From Figure 5.11 b), the diffraction peak of films containing 1, 3 and 5 wt% MMT/M$_3$T exhibits same three peaks at $2\theta = 2.10^{o}$, 4.40^{o} and 6.65^{o} corresponding to an interlayer spacing of 4.19, 1.99 and 1.35 nm, respectively in which increasing MMT/M$_3$T loading does not affect interlayer spacing of clay because MMT/M$_3$T has alkyl group which cannot be compatible with PLA's chain causing conventional composite. The results indicate that the diffraction peak shifts to lower angle when organoclay loading increases from 1 to 3 wt% but it shifts to higher angle when organoclay loading is over 3 wt%. This could be due to poor dispersion of organoclay in PLA matrix [19]. Furthermore, it was found that the interlayer spacing of PLA/MMT/M$_3$T films is higher than that of PLA/MMT/HT(OH)$_2$ films because MMT/M$_3$T exhibits wider interlayer spacing than the MMT/HT(OH)$_2$ [20].

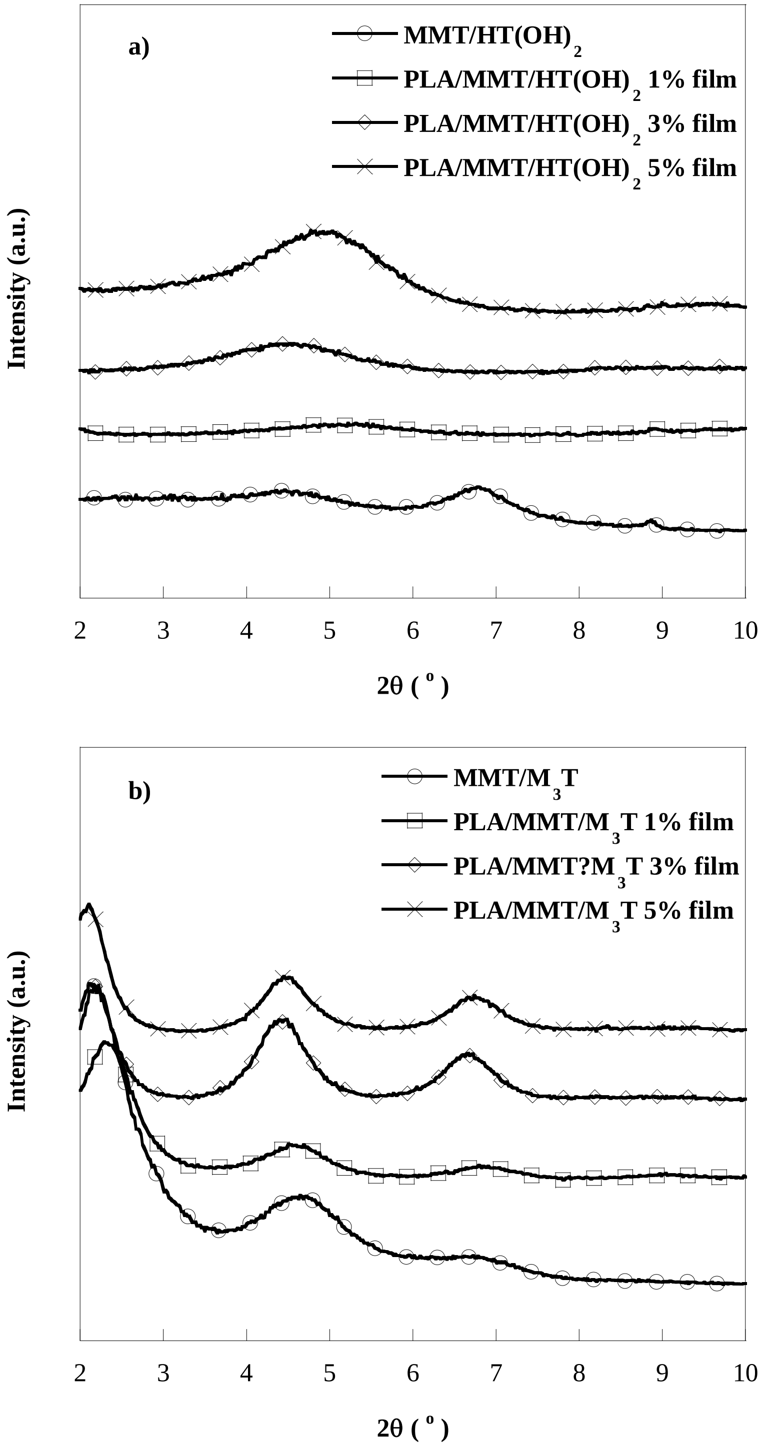

Figure 5.11 X-ray diffraction patterns of organoclay and nanocomposite films with different organoclay loading; a) MMT/HT(OH)$_2$ b) MMT/M$_3$T

5.3.2 Optical properties

Optical properties of plasticized PLA/organoclay nanocomposite films were investigated by optical transmittance measurement. The optical transmittance was recorded using a Lambda 650 Ultraviolet-visible spectrometer (UV–Vis) in the wavelength at 660 nm [20]. The transmittance of plasticized PLA blown films was continuously decreased with increasing organoclay loading which was shown in Figure 5.12. The decrease of transmittance is due to the hindrance of light passage by layer silicates of organoclay [20]. From XRD result, the interlayer spacing of MMT/HT(OH)$_2$ is smaller than that of MMT/M$_3$T causing the decreased transmittance of light. The data of optical properties are shown in table E.1 (Appendix E).

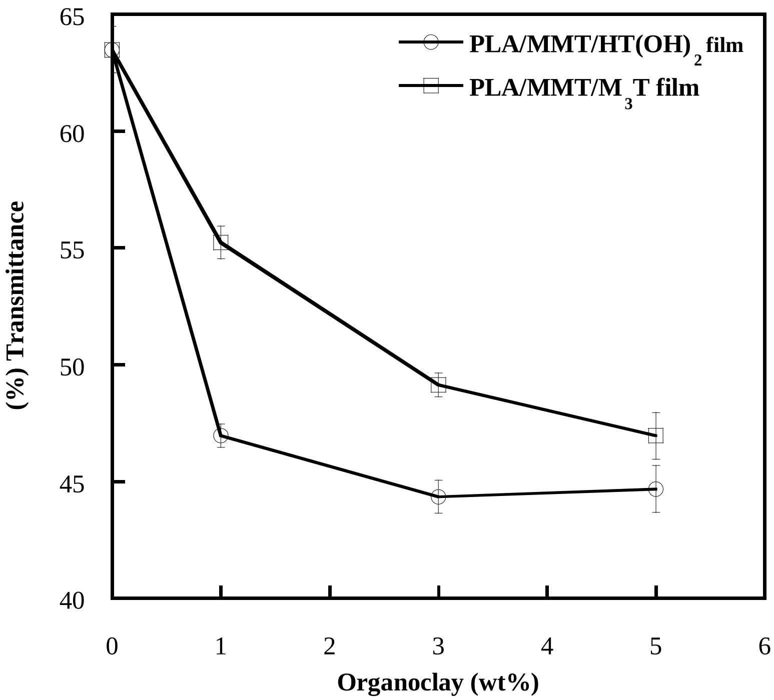

Figure 5.12 Ultraviolet-visible spectroscopy of plasticized PLA blown films with 1, 3 and 5 wt% organoclay: M$_3$T and HT(OH)$_2$

5.3.3 Thermal properties

Polymer/organoclay nanocomposites demonstrate better thermal property in comparison with neat polymer [19]. The effects of organoclay loading on the thermal properties in plasticized PLA/organoclay nanocomposite blown films are listed in table A.4 (Appendix A) and the DSC thermograms of the plasticized PLA blown films containing 1, 3 and 5 wt% of organoclay are shown in Figure 5.13. The T_{cc} of nanocomposite films decrease with increasing organoclay loading because the organoclay acts as a nucleating agent [11], but the T_g and T_m slightly change. Therefore, the organoclay loading does not significantly affect the T_m and T_g of PLA/organoclay nanocomposite films because PLA chain movement does not depend on the presence of organoclay [31]. Furthermore, the addition of organoclay into PLA matrix also increases degree of crystallinity of PLA/organoclay nanocomposite films as confirmed by area under T_{cc} and T_m peak. The addition of MMT/HT$(OH)_2$ gives higher degree of crystallinity than adding MMT/M_3T because intermolecular force between MMT/HT$(OH)_2$ and PLA molecular chain is stronger than MMT/M_3T [20]. The PLA/organoclay nanocomposite films exhibit two melting peaks at 143 and 154 ^{o}C, which represents the melting of α' and α crystalline phase of PLA respectively for all organoclay loading [5]. Moreover, α crystalline phase of PLA is still appeared for all organoclay loading while the area of melting peak of α' crystalline phase of PLA continuously decreases with increasing organoclay loading. It is attributed to the fact that increasing organoclay loading causes interlayer silicate form stacking which affects organoclay to have poor dispersion and hindering the crystal formation [19].

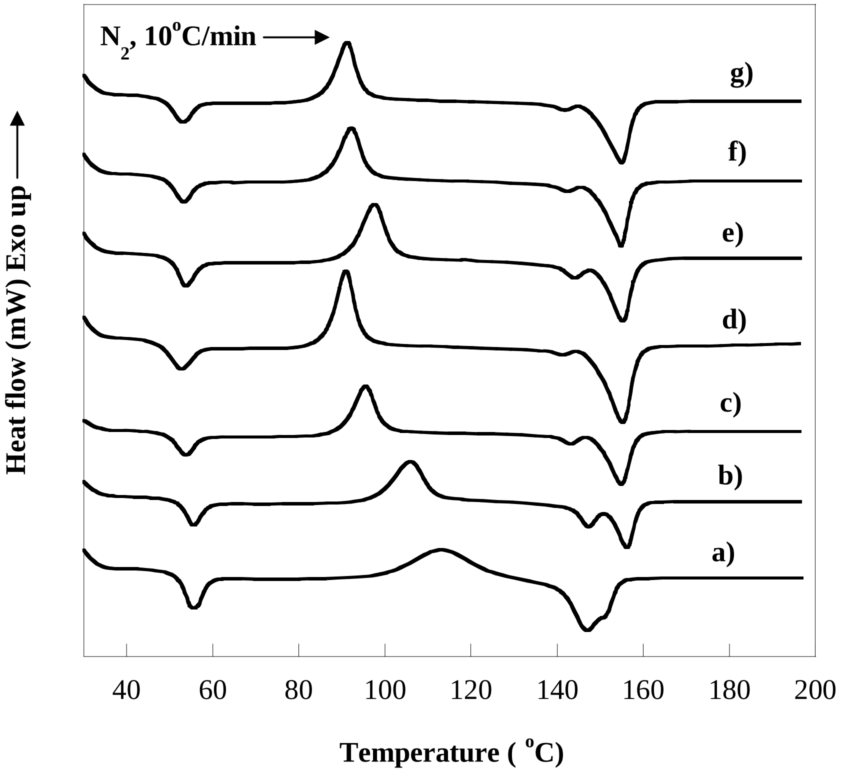

Figure 5.13 DSC thermograms recorded at a heating rate of 10 °C/min under N_2 for a) plasticized PLA 5 wt% PPG(1200); and PLA/MMT/HT(OH)$_2$ at b) 1 wt%, c) 3 wt%, d) 5 wt%; and PLA/MMT/M_3T at e) 1 wt%, f) 3 wt%, g) 5 wt%

5.3.4 Thermomechanical properties

Figure 5.14 a) presents the storage modulus of plasticized PLA nanocomposite blown films with different organoclay loading. The plasticized PLA/organoclay blown films exhibit higher storage modulus than that of plasticized PLA because the organoclay is a reinforcement agent [31]. At 30 ^{o}C the storage modulus of PLA/PPG blown film increases from 2000 to 2400-2600 MPa with increasing organoclay loading. The increase of storage modulus of film with organoclay in a range of 100 to 120 ^{o}C is due to the decreased T_c because organoclay behaves like nucleating agent resulting in easy to crystallization [11]. Furthermore, Figure 5.14 b) shows that there is no shift of tan δ peak even organoclay loading increases which indicated that there is no significant change of T_g of PLA/organoclay blown films because T_g depends on polymer's chain movement, molecular weight, crosslinking and intermolecular attraction which those affect movement of polymer chain [31]. However, incresing organoclay loading affects height of tan δ peak decreased because polymer chain can easily more which can increases degree of crystallinity. The data of thermomechanical properties and comparsion of T_g from thermal and thermomechanical results are displayed in table B.4 (Appendix B).

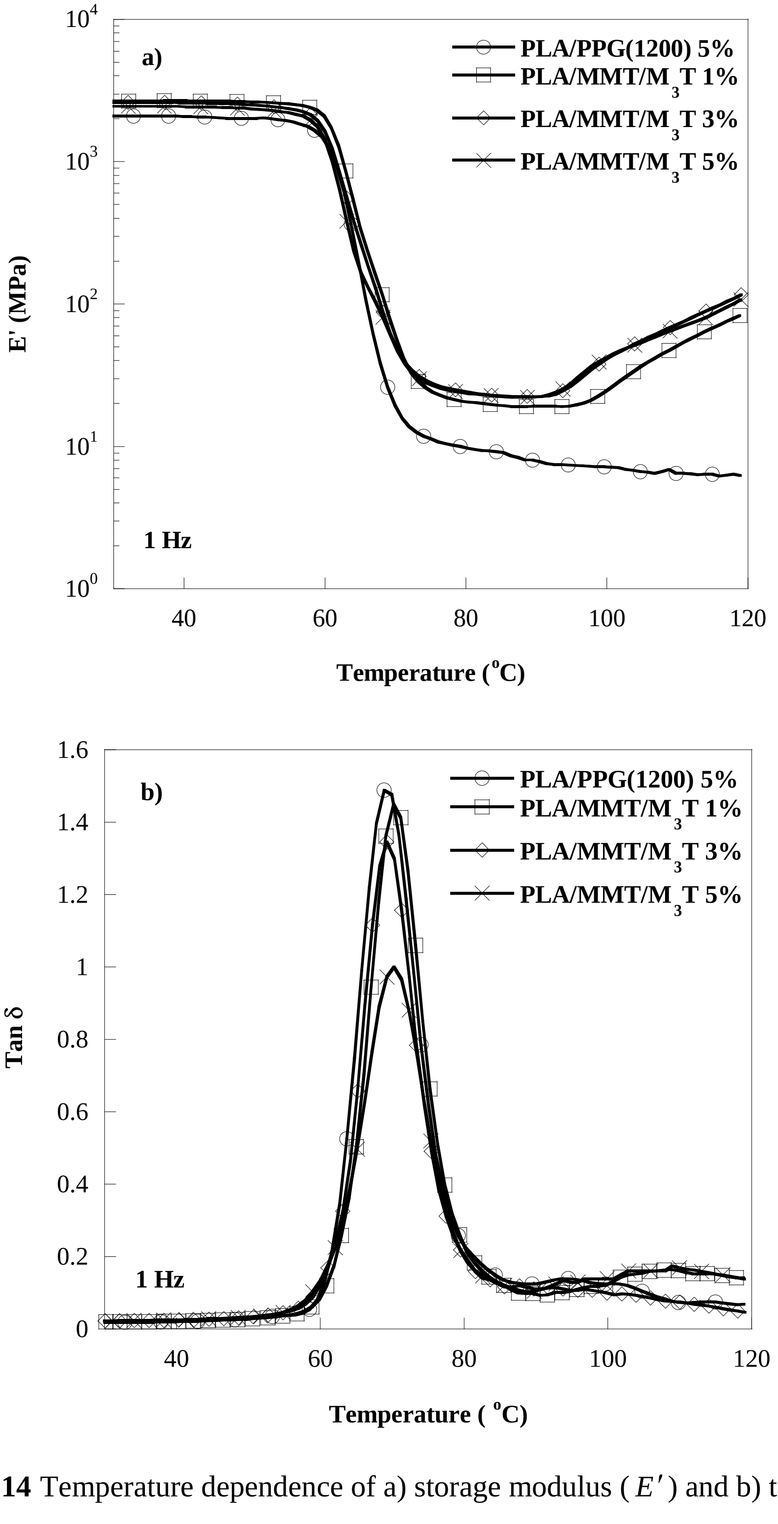

Figure 5.14 Temperature dependence of a) storage modulus (E') and b) tan δ for PLA containing 5 wt% PPG(1200) and plasticized PLA blown films with 1, 3 and 5 wt% MMT/M$_3$T

5.3.5 Mechanical properties

Tensile strength and tensile modulus of PLA/organoclay nanocomposite films increase with increasing organoclay loading which are shown in Figure 5.15 a) and b). Tensile strength and tensile modulus increase about 18-25 and 13-17 percentage, respectively when organoclay loading is 3 wt%. Then they decrease when 5 wt% organoclay is added into the system. At 5 wt% loading, the attractive force between the organoclay and PLA is disturbed by the stacking form of the organoclay. Furthermore, it was found that PLA/MMT/HT$(OH)_2$ film exhibits higher tensile strength and tensile modulus than PLA/MMT/M_3T film because HT$(OH)_2$ on clay's surface increases degree of crystallinity of PLA better than M_3T as shown in table C.4 (Appendix C). Moreover, HT$(OH)_2$ comprises of hydroxyl groups which increase hydrogen bonding [20]. In contrast, elongation at break of PLA/MMT/M_3T films, as shown in Figure 5.15 c), slightly decreases (about 25 percentage) when 3 wt% of MMT/M_3T is added. However, organoclay loading at 5 wt% leads to agglomeration of clay particles [32], which decreases the elongation at break of PLA film substantially (about 64 percentage). The same trend of elongation at break is also observed in PLA/MMT/HT$(OH)_2$. Furthermore, it was found that elongation at break of PLA/MMT/HT$(OH)_2$ film at the same organoclay content is lower than that with PLA/MMT/M_3T film because hydroxyl groups of MMT/HT$(OH)_2$ can be compatible PLA's chain causing higher surface attraction between polymer and clay. This leads to the difficulty in a PLA's chain movement.

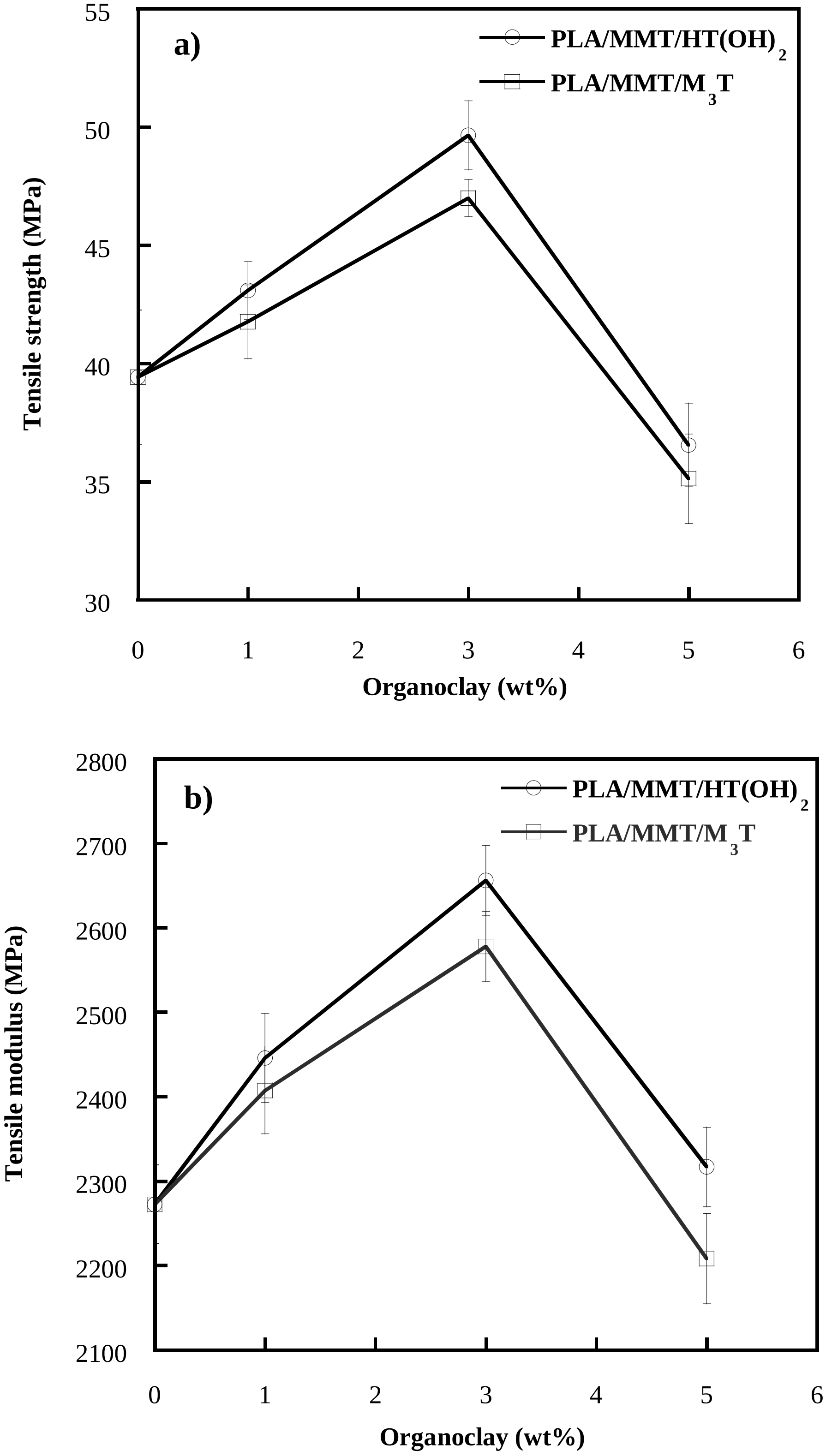
a)
PLA/MMT/HT(OH)$_2$
PLA/MMT/M$_3$T
Tensile strength (MPa)
55
50
45
40
35
30
0
1
2
3
4
5
6
Organoclay (wt%)
b)
PLA/MMT/HT(OH)$_2$
PLA/MMT/M$_3$T
Tensile modulus (MPa)
2800
2700
2600
2500
2400
2300
2200
2100
0
1
2
3
4
5
6
Organoclay (wt%)

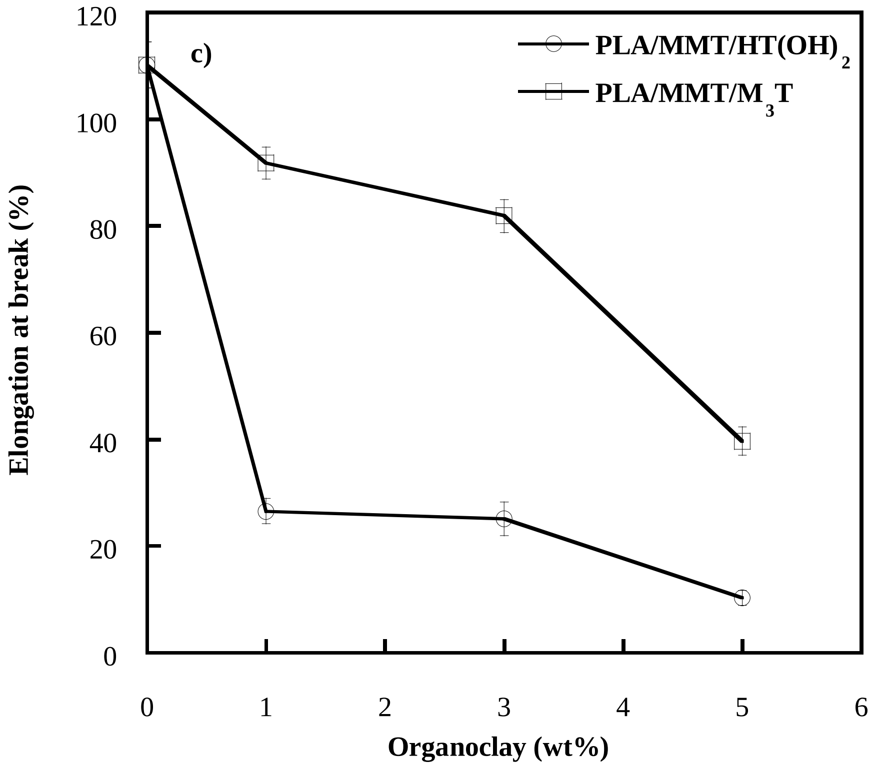

Figure 5.15 Mechanical properties of PLA blown films containing 5 wt% PPG(1200) and 1, 3 and 5 wt% of organoclay: M_3T and $HT(OH)_2$ a) tensile strength b) tensile modulus c) elongation at break

5.3.6 Barrier properties

The enhanced barrier performance of the nanocomposite films relative to the neat films depends on surface area, dispersion and polarity of the organoclay. Furthermore, the biaxial orientation of organoclay platelets in the polymer matrix produced during the blown film process increases tortuosity enough to produce enhanced barrier properties [18].

Oxygen and water vapor permeation of blown films containing 5 wt% PPG(1200) and 1, 3 and 5 wt% organoclay: M_3T and $HT(OH)_2$ are presented in Figure 5.16 a) and b), respectively. The oxygen permeation of PLA/MMT/$HT(OH)_2$ and PLA/MMT/M_3T films decrease around 24 and 17 percentage and water vapor permeation of PLA/MMT/$HT(OH)_2$ and PLA/MMT/M_3T films decrease around 8 and 14 percentage at 3 wt% MMT/$HT(OH)_2$ and MMT/M_3T loading respectively when compared with plasticized PLA blown film. The decrease of oxygen and water vapor permeability is mainly attributed to the dispersion of organoclay created the tortuous pathway where oxygen and water molecules must follow to permeate through film [18]. However, both organoclay increase oxygen permeability when clay loading is over 3 wt% because increasing organoclay loading causes agglomeration of silicate layer [20]. Additionally, it is found that PLA/MMT/$HT(OH)_2$ shows higher water vapor permeability compared to PLA/MMT/M_3T because of polarity of organoclay [20]. However PLA/MMT/$HT(OH)_2$ shows lower oxygen permeability compared to PLA/MMT/M_3T because it has less interlayer spacing. The data of barrier properties are shown in table F.1 and F.2 (Appendix F).

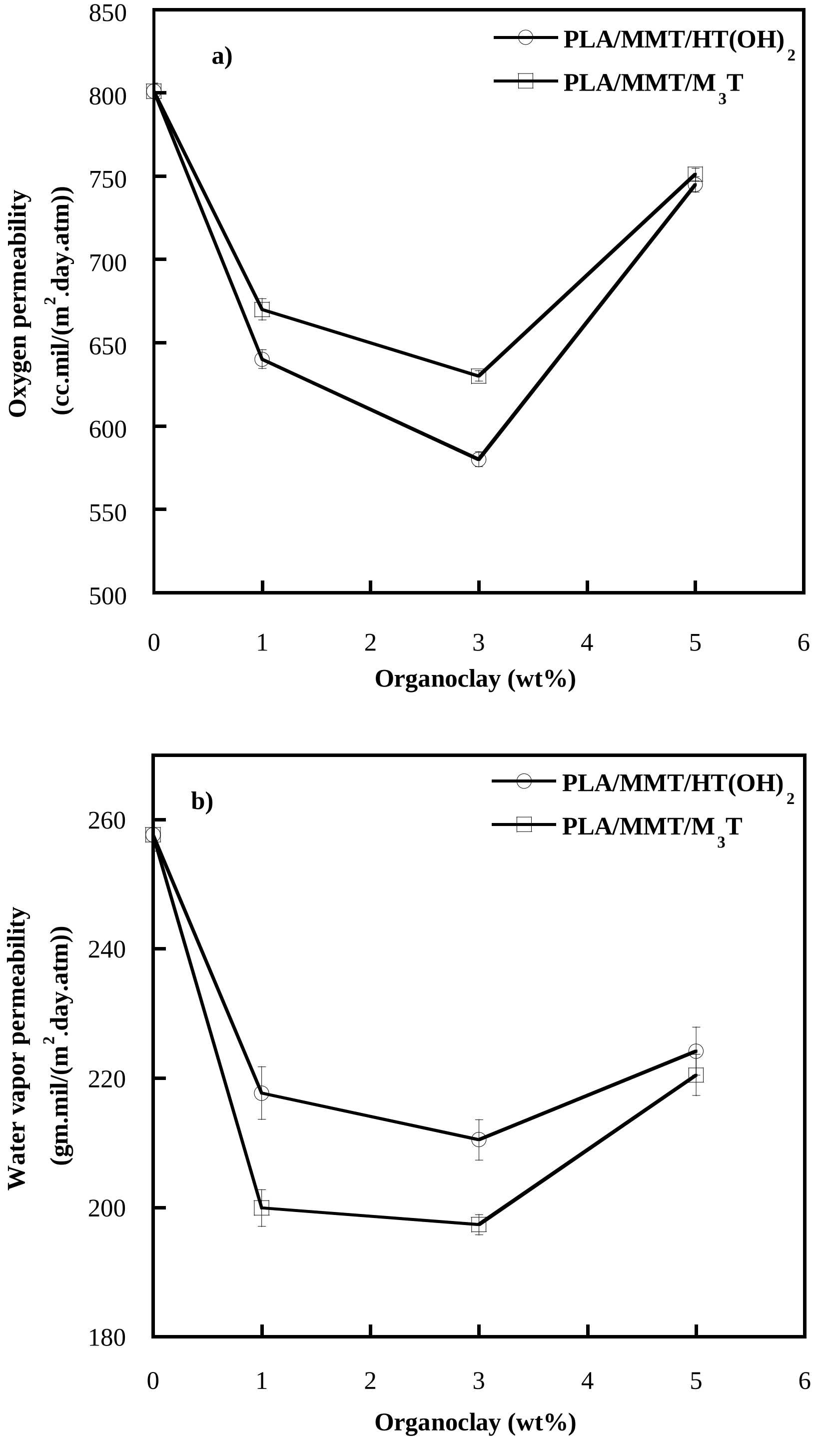

Figure 5.16 The permeability of PLA blown films containing 5 wt% PPG(1200) and 1, 3 and 5 wt% organoclay: M_3T and $HT(OH)_2$ a) oxygen and b) water vapor permeability

5.3.7 Oxygen permeation models

Many models have been used to predict gas permeation properties of plasticized PLA/organoclay blown films [33-35]. Here, oxygen was chosen as reference gas. Nielsen's model assumes that the barrier layers consist of ribbons contained within the polymer matrix. The ribbons have a width w, thickness t and are assumed to be perfectly aligned in the polymer matrix. Cussler (regular) model is used for perpendicular alignment of the ribbons to the direction of the permeating molecules and a smooth distribution of the ribbon. Cussler (random) model is used for randomness of alignment of ribbon structures in the polymer matrix. Bharadwaj model is an improvement of the Nielsen's model by incorporating an orientation parameter S. These models are shown as follows.

Nielsen's model:
$$R_p = \frac{1-\phi}{1+(\alpha\phi/2)}$$

Cussler (regular) model:
$$R_p = \frac{1-\phi}{1+(\alpha\phi/2)^2}$$

Cussler (random) model:
$$R_p = \frac{1-\phi}{1+(\alpha\phi/2)^3}$$

Bharadwaj model:
$$R_p = \frac{1-\phi}{1+(\alpha\phi(2S+1)/6)}$$

$$S = (3\cos^2\theta - 1)/2$$

R_p is relative permeability of polymer composite and polymer matrix, ϕ is the volume fraction of organoclay, $\alpha =$w/t is the aspect ratio of the ribbons. In this study, the aspect ratio of ribbon is approximately 100 according to the work done by Sun et al. [34]. S is introduced to quantify the degree of their orientation around the diffusion direction and θ is the angle between the direction of penetrated flow and the normal of the layers. $S = 0$ for random platelet orientation and $S = 1$ (Nielsen's model) for parallel orientation.

The oxygen permeation of plasticized PLA/organoclay blown films is compared by several gas permeation models as shown in Figure 5.17. Experimental result of plasticized PLA/MMT/HT$(OH)_2$ and PLA/MMT/M_3T at 1, 3 wt% is fitted Bharadwaj model than other models because fitting value ($R^2 = 0.969$) is better fitted with experimental result in which this model indicated that the ribbons possibly form a random array and non oriented. However, oxygen permeation of both organoclay at 5 wt% loading does not fitted well with any selected models, which might be due to the agglomeration of organoclay at high clay loading.

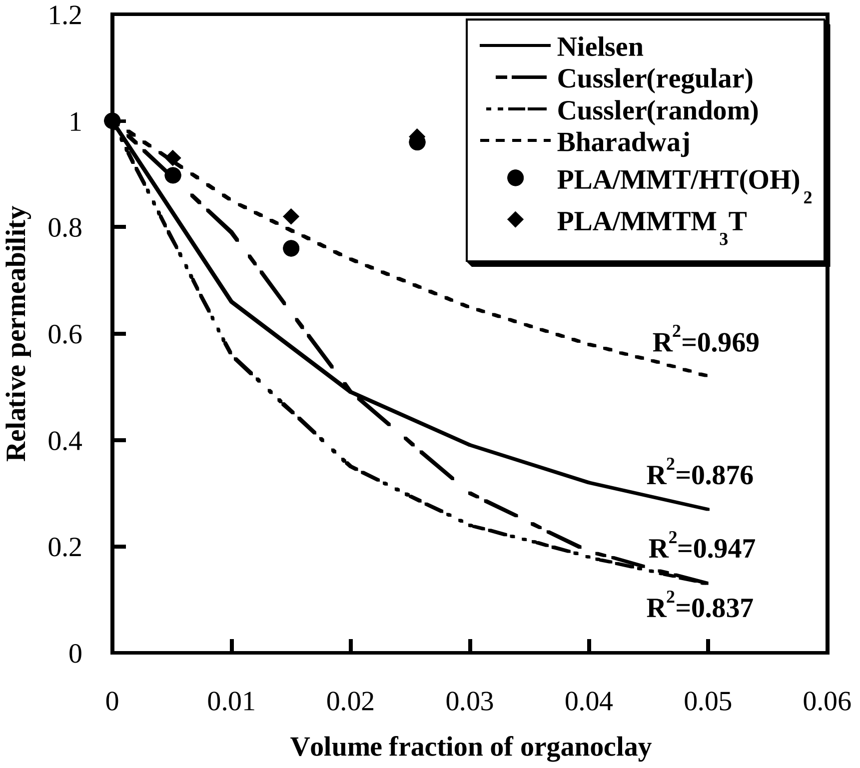

Figure 5.17 Comparison between experimental and models relative oxygen permeability of PLA blown films containing 5 wt% PPG(1200) and 1, 3 and 5 wt% organoclay: M_3T and $HT(OH)_2$

CHAPTER VI

CONCLUSIONS AND RECOMMENDATIONS

6.1 Conclusions

In first part, the effect of types and loading of plasticizer on properties of plasticized PLA blown films was studied. DSC and DMA results indicated that all plasticizers were compatible with PLA at 5 wt%. T_g and T_m of the plasticized PLA films shifted to lower temperature while increasing plasticizer content. In addition, the DSC peak of plasticized PLA appeared clearly which would be due to the increase in degree of crystallization. Tensile tests indicated that PPG was a suitable plasticizer for PLA which can be observed from an increase in elongation at break approximately 33 times.

In second part, we focused on the effect of the molecular weight of PPG on properties of plasticized PLA blown films. The experiment results indicated that MW influences the T_g. PLA mixing with high MW PPG, PPG(2000), exhibits two melting peaks. Furthermore, low MW PPG, PPG(1200), increases the elongation at break greater than high MW PPG.

In final part, surfactant types and organoclay loading on properties of PLA/clay nanocomposite blown films were also studied. From XRD result, it indicated that interlayer spacing of organoclay increased compared with pristine clay. Furthermore, MMT/M_3T had wider interlayer spacing than MMT/HT$(OH)_2$. However, PLA/MMT/M_3T film has clay dispersion form conventional composite and PLA/MMT/HT(OH)2 film has clay dispersion form intercalated nanocomposite.

Moreover, the addition of organoclay only affected T_c and also increased degree of crystallinity of blown films as confirmed by DSC and DMA. Furthermore, it was found that PLA/MMT/HT$(OH)_2$ films gave higher degree of crystallinity than PLA/MMT/M_3T films.

The improvement of mechanical and barrier properties of blowm films were evidenced by XRD, DSC and DMA data. From tensile tests, it was found that elongation at break of PLA/MMT/M_3T films was higher than that of PLA/MMT/HT$(OH)_2$ films and 3 wt% of organoclay loading showed optimum properties with plasticized PLA. Furthermore, a value of tensile strength still suffices for application in packaging field (value up to 24 MPa) [13]. In addition, PLA/MMT/HT$(OH)_2$ films showed higher water vapor permeation but lower oxygen permeation compared to PLA/MMT/M_3T films.

Finally, PLA film added PPG(1200) 5 wt% and MMT/M_3T 3 wt% showed optimum properties which can be observed from increasing tensile strength and tensile modulus about 21% and 14%, respectively but elongation at break decreases about 25%. Furthermore, this film decreases water vapor permeation and oxygen permeation about 23% and 21%, respectively.

6.2 Recommendations

The incorporation of additives in form of solid (such as adipic acid) and liquid (such as PPG) before melt mixing through the extruder should be contained in the individually separated hoppers and feeding rate should be controlled automatically instead of mixing with PLA pellet with those manually before adding to the extruder.

REFERENCES

[1] Lim, L. T.; Auras, R.; and Rubino, M. Processing technologies for poly(lactic acid). Progress in Polymer Science (2008): 820-852.

[2] Henton, D. E.; Gruber, P.; Lunt, J.; and Randall, J. Polylactic Acid Technology. Natural Fibers, Biopolymers, and Biocomposites (2005): 528-569.

[3] Piorkowska, E.; Kulinski, Z.; Galeski, A.; and Masirek, R. Plasticization of semicrystalline poly(L-lactide) with poly(propylene glycol). Polymer 47 (2006): 7178-7188.

[4] Kulinski, Z.; Piorkowska, E.; Gadzinowska, K.; and Stasiak, M. Plasticization of Poly(L-lactide) with Poly(propylene glycol). Biomacromolecules (2006): 2128-2135.

[5] Jia, Z.; Tan, J.; Han, C.; Yang, Y.; and Dong, L. Poly(ethylene glycol-co-propylene glycol) as a Macromolecular Plasticizing Agent for Polylactide: Thermomechanical Properties and Aging. Journal of Applied Polymer Science (2009): 1105-1117.

[6] Wypych, G. Handbook of plasticizers. New York: Chemtec laboratories, Inc, 2004.

[7] Howick, C. Chemistry Review. 5 ed. Vol. 4. University of York (UK): Taylor and Francis group, 1993.

[8] Choudalakis, G.; and Gotsis, A. D. Permeability of polymer/clay nanocomposites: A review. European Polymer Journal (2009): 967-984.

[9] Pusch, R.; and Yong, R. N. Microstructure of Smectite Clays and Engineering Performance. New York: Taylor and Francis group, 2004.

[10] Huneault, M. A.; and Li, H. Morphology and properties of compatibilized polylactide/ thermoplastic starch blends. Polymer (2007): 270-280.

[11] Ray, S. S., et al. New polylactide/layered silicate nanocomposites. 5. Designing of materials with desired properties. Polymer (2003): 6633-6646.

[12] Riaz, M. N. Extruders in Food Applications. USA: Taylor and Francis group, 2000.

[13] Lemmouchi, Y., et al. Plasticization of poly(lactide) with blends of tributyl citrate and low molecular weight poly(D,L-lactide)-b-poly(ethylene glycol) copolymers. European Polymer 45 (2009): 2839–2848.

[14] Ljungberg, N.; and Wesslen, B. Tributyl citrate oligomers as plasticizers for poly (lactic acid): thermo-mechanical film properties and aging. Polymer 44 (2003): 7679-7688.

[15] Yang, S. L.; Wu, Z. H.; Meng, B.; and Yang, W. The Effects of Dioctyl Phthalate Plasticization on the Morphology and Thermal, Mechanical, and Rheological Properties of Chemical Crosslinked Polylactide. Journal of Applied Polymer Science 3 (2009): 1136-1145.

[16] Zenkiewicz, M.; and Richert, J. Permeability of polylactide nanocomposite films for water vapour, oxygen and carbon dioxide. Polymer Testing (2008): 835-840.

[17] Paul, M. A., et al. New nanocomposite materials based on plasticized poly(L-lactide) and organo-modified montmorillonites: thermal and morphological study. Polymer (2003): 443-450.

[18] Thellen, C., et al. Influence of montmorillonite layered silicate on plasticized poly(L-lactide) blown films. Polymer (2005): 11716-11727.

[19] Xuanjun, W.; Jizu, Y.; Yongfu, Y.; and Yanxiong, W. Preparation and Characterization of Polylactide/Montmorillonite Nanocomposites. 24 562-565.

[20] Rhim, J. W.; Hong, S. I.; and Ha, C. S. Tensile, water vapor barrier and antimicrobial properties of PLA/nanoclay composite films. LWT-Food Science and Technology (2009): 612-617.

[21] Pluta, M.; Jeszka, J. K.; and Boiteux, G. Polylactide/montmorillonite nanocomposites: Structure, dielectric, viscoelastic and thermal properties. European Polymer Journal (2007): 2819-2835.

[22] He, H.; Ma, Y.; Zhu, J.; Yuan, P.; and Qing, Y. Organoclays prepared from montmorillonites eith different cation exchange capacity and surfactant configuration. Applied Clay Science (2010): 67-72.

[23] Cho, J. W.; and Paul, D. R. Nylon 6 nanocomposites by melt compounding. Polymer (2001): 1083-1094.

[24] Lopez, D. G.; Picazo, O.; Merino, J. C.; and Pastor, J. M. Polypropylene-clay nanocomposites: effect of compatibilizing agents on clay dispersion. European Polymer Journal (2003): 945-950.

[25] Gopakumar, T. G.; Lee, J. A.; Kontopoulou, M.; and Parent, J. S. Influence of clay exfoliation on the physical properties of montmorillonite/polyethylene composites. Polymer (2002): 5483-5491.

[26] Pan, P.; and Inoue, Y. Polymorphism and isomorphism in biodegradable polyesters. Progress in Polymer Science (2009): 605-640.

[27] Auras, R.; Lim, L.-T.; Selke, S. E. M.; and Tsuji, H. Poly(lactic acid): Synthesis, Structures, Properties, Processing, and Applications. Canada: Wiley & Sons, Inc, 2010.

[28] Cocca, M.; Lorenz, M. L. D.; Malinconico, M.; and Frezza, V. Influence of crystal polymorphism on mechanical and barrier properties of poly(L-lactic acid). European Polymer Journal (2011): 1-8.

[29] US patent 7,632,897B2. Matsumoto, et al. Polylactic acid base polymer composition, molding thereof and film. issued 2009-12-15.

[30] Utracki, L. A. Clay-Containing Polymeric Nanocomposites. Vol. 1. United Kingdom: Rapra Technology Limited, 2004.

[31] Chow, W. S.; and Lok, S. K. Thermal properties of poly(lactic acid)/organo-montmorillonite nanocomposites. Thermal Analysis and Calorimetry 95 (2009): 627-632.

[32] Chang, J. H.; An, Y. U.; Cho, D.; and Giannelis, E. P. Poly(lactic acid) nanocomposites: coparison of their properties with montmorillonite and synthetic mica (II). Polymer 44 (2003): 3715-3720.

[33] Lu, C.; and Mai, Y. W. Permeability modelling of polymer-layered silicate nanocomposites. Composites Science and Technology 67 (2007): 2895-2902.

[34] Sun, L.; Boo, W.-J.; Clearfield, A.; Sue, H.-J.; and Pham, H. Q. Barrier properties of model epoxy nanocomposites. Membrane Science (2008): 129-136.

[35] Bhattaacharya, M.; Biswas, S.; and Bhowmick, A. K. Permeation characteristics and modeling of barrier properties of multifunctional rubber nanocomposites. Polymer 52 (2011): 1562-1576.

APPENDICES

Appendix A

Data of thermal properties

Table A.1 Thermal properties and the degree of crystallinity of neat PLA and the plasticized PLA with 3, 5 and 7 wt% of plasticizers

Plasticizer type	**Plasticizer content (wt %)**	**T_g (°C)**	**T_{cc} (°C)**	**ΔH_c (J/g)**	**T_m (°C)**	**ΔH_m (J/g)**	**X_c (%)**
None	0	63.03	124.48	2.01	153.44	3.09	1.16
Adipic acid	3	56.93	102.23	29.17	142.43, 151.17	31.04	2.07
	5	51.94	91.81	34.26	141.32, 146.84	42.13	8.91
	7	55.90	91.74	26.01	142.47, 151.67	45.87	22.96
PPG(1200)	3	57.01	121.59	12.32	149.16	14.07	1.94
	5	53.24	113.33	22.96	147.06	25.27	2.61
	7	49.83	105.07	24.09	155.62	29.11	5.80
DOP	3	58.93	120.29	23.24	150.78	24.25	1.12
	5	52.63	122.75	16.54	149.44	17.80	1.43
	7	48.94	116.72	18.79	147.53	20.34	1.79
TBC	3	57.97	121.55	21.99	151.46	22.99	1.11
	5	54.36	116.92	24.02	149.38	25.39	1.32
	7	47.20	109.93	30.49	153.25	31.71	1.41
PEPG	3	57.38	122.64	4.12	148.93	5.15	1.14
	5	52.88	109.23	24.08	156.25	26.59	2.84
	7	49.18	101.03	28.97	156.22	31.74	5.52

Table A.2 Thermal properties and the degree of crystallinity of neat PLA and the plasticized PLA with 3, 5 and 7 wt% of plasticizers (PPG group)

Plasticizer type	**Plasticizer content (wt %)**	**T_g (^oC)**	**T_{cc} (^oC)**	**ΔH_c (J/g)**	**T_m (^oC)**	**ΔH_m (J/g)**	**X_c (%)**
None	0	63.03	124.48	2.01	153.44	3.09	1.16
PPG(1200)	3	57.01	121.59	12.32	149.16	14.07	1.94
	5	53.24	113.33	22.96	147.06	25.27	2.61
	7	49.83	105.07	24.09	146.58, 155.62	29.11	5.80
PPG(2000)	3	58.36	112.92	21.24	150.34, 155.95	22.80	1.73
	5	57.17	107.71	22.61	150.88, 155.79	24.65	2.31
	7	56.46	106.94	23.67	149.31, 154.59	28.00	5.01

Table A.3 Thermal properties and the degree of crystallinity of neat PLA and the plasticized PLA with 3, 5 and 7 wt% of plasticizers (acid group)

Plasticizer type	**Plasticizer content (wt %)**	**T_g (^oC)**	**T_{cc} (^oC)**	**ΔH_c (J/g)**	**T_m (^oC)**	**ΔH_m (J/g)**	**X_c (%)**
None	0	63.03	124.48	2.01	153.44	3.09	1.16
Adipic acid	3	56.93	102.23	29.17	142.43, 151.17	31.04	2.07
	5	51.94	91.81	34.26	141.32, 146.84	42.13	8.91
	7	55.90	91.74	26.01	142.47, 151.67	45.87	22.96
Sebacic acid	3	53.90	99.62	21.74	147.11, 154.26	23.02	1.42
	5	49.21	90.61	22.37	145.87, 150.52	27.69	6.02
	7	52.88	85.34	20.70	146.35, 150.75	28.99	9.58
Dodecanedioic acid	3	55.41	100.26	21.03	148.00, 154.39	22.45	1.57
	5	49.57	91.84	21.73	146.92, 152.24	26.83	5.77
	7	53.07	84.74	20.01	146.11, 151.73	27.87	9.09

Table A.4 Thermal properties and the degree of crystallinity of PLA/PPG(1200) 5 wt% and the plasticized PLA/organoclay with 1, 3 and 5 wt% of organoclays

Organoclay type	**Organoclay loading (wt %)**	**T_g (°C)**	**T_{cc} (°C)**	**ΔH_c (J/g)**	**T_m (°C)**	**ΔH_m (J/g)**	**X_c (%)**
None (PLA/PPG(1200) 5wt%)	0	53.24	113.33	22.96	147.06	25.27	2.61
MMT/HT(OH)$_2$	1	53.25	105.88	22.04	149.67, 156.23	26.94	5.61
	3	51.23	95.44	20.19	154.99	26.84	7.77
	5	50.83	90.92	23.21	155.31	27.13	4.68
MMT/M$_3$T	1	51.62	97.45	22.42	148.41, 155.40	25.75	3.80
	3	50.66	92.17	21.05	154.88	26.14	5.95
	5	50.53	91.24	24.35	155.06	26.89	3.03

Appendix B

Data of thermomechanical properties

Table B.1 Thermomechanical properties of neat PLA and the plasticized PLA with 3, 5 and 7 wt% of plasticizers

Plasticizer type	Plasticizer content (wt %)	Storage modulus (MPa)	E' T_g (^oC)	tan δ T_g (^oC)
None	0	2800.08	76.50	80.10
Adipic acid	3	2285.10	68.88	75.75
	5	2020.00	67.22	72.25
	7	2618.94	69.15	76.25
PPG(1200)	3	2166.08	69.25	73.25
	5	2009.56	65.25	69.00
	7	1832.41	62.20	66.00
DOP	3	2322.33	69.00	73.25
	5	2301.00	64.50	67.75
	7	2120.59	61.00	64.50
TBC	3	2035.26	69.75	73.50
	5	1974.67	65.71	68.70
	7	1897.93	59.55	65.50
PEPG	3	2378.44	69.30	72.80
	5	2114.44	67.00	70.55
	7	1919.46	64.50	66.78

Table B.2 Thermomechanical properties of neat PLA and the plasticized PLA with 3, 5 and 7 wt% of plasticizers (PPG group)

Plasticizer type	**Plasticizer content (wt %)**	**Storage modulus (MPa)**	E' **T_g (^oC)**	**tan** δ **T_g (^oC)**
None	0	2800.08	76.50	80.10
PPG(1200)	3	2166.08	69.25	73.25
	5	2009.56	65.25	69.00
	7	1832.41	62.20	66.00
PPG(2000)	3	2214.56	71.50	75.10
	5	2000.92	71.00	74.60
	7	1877.26	70.25	74.00

Table B.3 Thermomechanical properties of neat PLA and the plasticized PLA with 3, 5 and 7 wt% of plasticizers (acid group)

Plasticizer type	Plasticizer content (wt %)	Storage modulus (MPa)	E' T$_g$ (^{o}C)	tan δ T$_g$ (^{o}C)
None	0	2800.08	76.50	80.10
Adipic acid	3	2285.10	68.88	75.75
	5	2020.00	67.22	72.25
	7	2618.94	69.15	76.25
Sebacic acid	3	2220.18	67.78	74.08
	5	2014.66	65.25	70.30
	7	2232.41	68.20	74.50
Dodecanedioic acid	3	2172.20	67.18	73.58
	5	1954.26	65.53	71.06
	7	2285.76	68.94	75.10

Table B.4 Thermomechanical properties of PLA/PPG(1200) 5 wt% and the plasticized PLA/organoclay with 1, 3 and 5 wt% of organoclays

Organoclay type	**Organoclay loading (wt %)**	**Storage modulus (MPa)**	E' **T_g (^oC)**	**tan** δ **T_g (^oC)**
None (PLA/PPG(1200) 5wt%)	0	2009.56	65.25	69.00
MMT/HT(OH)$_2$	1	2706.08	65.63	69.79
	3	2649.51	64.87	69.20
	5	2523.24	64.55	68.96
MMT/M$_3$T	1	2658.16	65.20	70.00
	3	2600.33	65.12	69.21
	5	2441.41	64.80	69.55

Appendix C

Data of mechanical properties

Table C.1 Mechanical properties in MD of neat PLA

No.	Tensile strength (MPa)	Tensile modulus (MPa)	Elongation at break (%)
1	61.29	3023.93	3.31
2	53.34	2695.63	3.83
3	61.10	3047.55	3.25
4	61.30	3026.10	3.15
5	52.34	2637.03	3.18
Avg	57.87	2886.05	3.34
SD	4.12	180.54	0.25

Table C.2 Mechanical properties in TD of neat PLA

No.	Tensile strength (MPa)	Tensile modulus (MPa)	Elongation at break (%)
1	47.71	2803.19	2.26
2	49.58	2966.10	1.96
3	45.10	2698.69	2.22
4	44.98	2785.05	1.98
5	49.70	2966.03	2.32
Avg	47.41	2843.81	2.15
SD	2.06	105.88	0.15

Table C.3 Mechanical properties in MD of PLA/Adipic acid 3 wt%

No.	Tensile strength (MPa)	Tensile modulus (MPa)	Elongation at break (%)
1	50.54	2818.60	2.67
2	47.27	2649.94	2.89
3	47.83	2674.38	2.99
4	48.01	2688.74	3.19
5	43.34	2459.50	2.65
Avg	47.40	2658.23	2.88
SD	2.32	115.30	0.20

Table C.4 Mechanical properties in TD of PLA/Adipic acid 3 wt%

No.	Tensile strength (MPa)	Tensile modulus (MPa)	Elongation at break (%)
1	34.83	2685.19	1.63
2	34.05	2586.95	1.59
3	34.76	2610.56	1.50
4	34.69	2695.68	1.50
5	31.15	2582.64	1.50
Avg	33.90	2632.20	1.54
SD	1.40	48.60	0.06

Table C.5 Mechanical properties in MD of PLA/Adipic acid 5 wt%

No.	Tensile strength (MPa)	Tensile modulus (MPa)	Elongation at break (%)
1	34.76	2204.93	7.41
2	42.23	2240.77	6.28
3	53.15	2485.30	5.42
4	43.17	2305.23	6.55
5	33.82	2172.28	7.95
Avg	41.43	2281.70	6.72
SD	6.98	110.95	0.88

Table C.6 Mechanical properties in TD of PLA/Adipic acid 5 wt%

No.	Tensile strength (MPa)	Tensile modulus (MPa)	Elongation at break (%)
1	30.50	2228.72	1.61
2	27.45	2151.97	1.59
3	29.29	2200.56	1.42
4	24.42	2038.53	1.44
5	28.93	2187.67	1.56
Avg	28.12	2161.49	1.52
SD	2.09	66.25	0.08

Table C.7 Mechanical properties in MD of PLA/Adipic acid 7 wt%

No.	Tensile strength (MPa)	Tensile modulus (MPa)	Elongation at break (%)
1	52.57	2808.05	2.20
2	53.27	2879.00	2.44
3	52.51	2829.04	2.44
4	52.44	2784.33	2.42
5	50.97	2752.80	2.41
Avg	52.35	2810.64	2.38
SD	0.75	42.56	0.09

Table C.8 Mechanical properties in TD of PLA/Adipic acid 7 wt%

No.	Tensile strength (MPa)	Tensile modulus (MPa)	Elongation at break (%)
1	28.15	2488.72	1.50
2	28.61	2511.97	1.49
3	28.98	2542.56	1.39
4	32.11	2600.53	1.40
5	34.46	2647.67	1.44
Avg	30.46	2558.29	1.44
SD	2.44	58.32	0.04

Table C.9 Mechanical properties in MD of PLA/PPG(1200) 3 wt%

No.	Tensile strength (MPa)	Tensile modulus (MPa)	Elongation at break (%)
1	50.21	2652.59	22.32
2	51.11	2687.96	23.81
3	40.49	2370.08	18.26
4	44.60	2491.47	22.96
5	44.6	2491.47	22.96
Avg	46.20	2538.71	22.06
SD	3.95	116.74	1.96

Table C.10 Mechanical properties in TD of PLA/PPG(1200) 3 wt%

No.	Tensile strength (MPa)	Tensile modulus (MPa)	Elongation at break (%)
1	37.92	2355.76	2.38
2	38.08	2490.42	2.23
3	39.69	2510.00	2.12
4	38.02	2456.84	2.24
5	38.02	2456.84	2.24
Avg	38.35	2453.97	2.24
SD	0.67	53.16	0.08

Table C.11 Mechanical properties in MD of PLA/PPG(1200) 5 wt%

No.	Tensile strength (MPa)	Tensile modulus (MPa)	Elongation at break (%)
1	39.76	2308.27	112.94
2	35.55	2070.1	104.32
3	36.93	2200.88	105.74
4	42.98	2434.82	115.57
5	41.89	2347.96	112.29
Avg	39.42	2272.41	110.17
SD	2.83	126.03	4.36

Table C.12 Mechanical properties in TD of PLA/PPG(1200) 5 wt%

No.	Tensile strength (MPa)	Tensile modulus (MPa)	Elongation at break (%)
1	29.36	2213.57	6.51
2	29.28	2250.14	5.31
3	27.73	2100.38	6.4
4	26.9	2084.32	7.69
5	27.73	2100.38	6.4
Avg	28.20	2149.76	6.46
SD	0.96	68.27	0.75

Table C.13 Mechanical properties in MD of PLA/PPG(1200) 7 wt%

No.	Tensile strength (MPa)	Tensile modulus (MPa)	Elongation at break (%)
1	34.48	2156.41	147.47
2	36.38	2110.38	161.33
3	35.86	2197.56	154.64
4	32.02	2100.67	144.7
5	32.42	2094.34	144.96
Avg	34.23	2131.87	150.62
SD	1.76	39.40	6.45

Table C.14 Mechanical properties in TD of PLA/PPG(1200) 7 wt%

No.	Tensile strength (MPa)	Tensile modulus (MPa)	Elongation at break (%)
1	27.27	2165.36	15.38
2	25.21	2007.06	13.93
3	25.67	2087.11	15.16
4	25.72	2096.9	12.7
5	24.42	1995.78	10.33
Avg	25.66	2070.44	13.50
SD	0.93	62.58	1.85

Table C.15 Mechanical properties in MD of PLA/DOP 3 wt%

No.	Tensile strength (MPa)	Tensile modulus (MPa)	Elongation at break (%)
1	47.56	2620.4	2.65
2	51.93	2858.53	2.7
3	51.36	2804.89	2.74
4	46.83	2558.16	2.5
5	50.06	2751.74	3.15
Avg	49.55	2718.74	2.75
SD	2.03	112.70	0.22

Table C.16 Mechanical properties in TD of PLA/DOP 3 wt%

No.	Tensile strength (MPa)	Tensile modulus (MPa)	Elongation at break (%)
1	34.4	2555.76	1.59
2	33.9	2490.42	1.64
3	31.38	2410.00	1.64
4	29.35	2400.84	1.57
5	31.55	2456.84	1.51
Avg	32.12	2462.77	1.59
SD	1.84	56.69	0.05

Table C.17 Mechanical properties in MD of PLA/DOP 5 wt%

No.	Tensile strength (MPa)	Tensile modulus (MPa)	Elongation at break (%)
1	45.14	2512.43	3.14
2	47.80	2686.71	3.81
3	36.82	2026.96	3.27
4	46.70	2621.07	3.36
5	46.83	2680.45	3.37
Avg	44.66	2505.52	3.39
SD	4.01	247.33	0.23

Table C.18 Mechanical properties in TD of PLA/DOP 5 wt%

No.	Tensile strength (MPa)	Tensile modulus (MPa)	Elongation at break (%)
1	29.81	2445.76	1.57
2	29.57	2420.42	1.48
3	29.38	2387.32	1.54
4	28.58	2302.14	1.53
5	29.61	2436.84	1.45
Avg	29.39	2398.50	1.51
SD	0.43	52.14	0.04

Table C.19 Mechanical properties in MD of PLA/DOP 7 wt%

No.	Tensile strength (MPa)	Tensile modulus (MPa)	Elongation at break (%)
1	42.91	2373.59	5.03
2	43.26	2212.10	3.59
3	47.02	2461.81	4.46
4	42.72	2240.28	5.92
5	42.32	2334.21	4.77
Avg	43.65	2324.40	4.75
SD	1.71	90.65	0.76

Table C.20 Mechanical properties in TD of PLA/DOP 7 wt%

No.	Tensile strength (MPa)	Tensile modulus (MPa)	Elongation at break (%)
1	29.78	2331.46	1.6
2	29.11	2288.32	1.56
3	29.52	2300.32	1.77
4	29.12	2271.84	1.67
5	28.14	2236.84	1.58
Avg	29.13	2285.76	1.64
SD	0.56	31.29	0.08

Table C.21 Mechanical properties in MD of PLA/TBC 3 wt%

No.	Tensile strength (MPa)	Tensile modulus (MPa)	Elongation at break (%)
1	46.22	2604.70	2
2	45.73	2523.96	2.41
3	49.8	2797.29	2.23
4	48.52	2732.66	3.78
5	43.96	2451.12	3.43
Avg	46.85	2621.95	2.77
SD	2.07	128.13	0.70

Table C.22 Mechanical properties in TD of PLA/TBC 3 wt%

No.	Tensile strength (MPa)	Tensile modulus (MPa)	Elongation at break (%)
1	34.5	2356.11	1.66
2	34.13	2315.28	1.54
3	34.72	2373.76	1.37
4	35.81	2487.70	1.85
5	35.91	2500.80	1.82
Avg	35.01	2406.73	1.65
SD	0.72	74.05	0.18

Table C.23 Mechanical properties in MD of PLA/TBC 5 wt%

No.	Tensile strength (MPa)	Tensile modulus (MPa)	Elongation at break (%)
1	42.92	2344.70	3.08
2	43.36	2423.96	3.21
3	43.40	2471.12	3.68
4	44.62	2582.66	3.07
5	44.64	2557.29	3.50
Avg	43.79	2475.95	3.31
SD	0.71	87.13	0.24

Table C.24 Mechanical properties in TD of PLA/TBC 5 wt%

No.	Tensile strength (MPa)	Tensile modulus (MPa)	Elongation at break (%)
1	34.48	2416.11	2.22
2	34.65	2315.20	1.92
3	34.65	2373.76	2.35
4	34.84	2337.57	2.29
5	34.27	2300.00	2.38
Avg	34.58	2348.53	2.23
SD	0.19	41.93	0.17

Table C.25 Mechanical properties in MD of PLA/TBC 7 wt%

No.	Tensile strength (MPa)	Tensile modulus (MPa)	Elongation at break (%)
1	41.24	2304.44	3.15
2	40.80	2213.67	3.24
3	42.70	2409.27	4.27
4	42.24	2357.83	3.31
5	40.73	2200.81	3.07
Avg	41.54	2297.20	3.41
SD	0.79	80.69	0.44

Table C.26 Mechanical properties in TD of PLA/TBC 7 wt%

No.	Tensile strength (MPa)	Tensile modulus (MPa)	Elongation at break (%)
1	35.18	2396.01	2.33
2	34.27	2355.23	2.47
3	35.03	2373.76	2.33
4	33.07	2207.89	2.29
5	34.01	2210.00	2.17
Avg	34.31	2308.58	2.32
SD	0.76	82.37	0.10

Table C.27 Mechanical properties in MD of PLA/PEPG 3 wt%

No.	Tensile strength (MPa)	Tensile modulus (MPa)	Elongation at break (%)
1	47.97	2667.79	2.9
2	45.87	2547.69	2.86
3	47.64	2501.36	2.77
4	45.67	2475.99	2.71
5	48.75	2707.07	2.63
Avg	47.18	2579.98	2.77
SD	1.21	91.54	0.10

Table C.28 Mechanical properties in TD of PLA/PEPG 3 wt%

No.	Tensile strength (MPa)	Tensile modulus (MPa)	Elongation at break (%)
1	36.55	2517.59	1.92
2	33.87	2323.70	1.85
3	33.95	2342.65	1.81
4	34.13	2398.54	1.74
5	31.8	2276.98	1.61
Avg	34.06	2371.89	1.79
SD	1.51	82.61	0.11

Table C.29 Mechanical properties in MD of PLA/PEPG 5 wt%

No.	Tensile strength (MPa)	Tensile modulus (MPa)	Elongation at break (%)
1	42.77	2339	5.93
2	40.53	2381.8	5.72
3	41.65	2303.34	6.8
4	44.02	2351.22	8.14
5	42.5	2398.11	9.01
Avg	42.29	2354.69	7.12
SD	1.16	33.21	1.27

Table C.30 Mechanical properties in TD of PLA/PEPG 5 wt%

No.	Tensile strength (MPa)	Tensile modulus (MPa)	Elongation at break (%)
1	33.73	2313.29	1.75
2	33.33	2300.70	1.81
3	31.44	2242.87	1.87
4	33.79	2358.75	1.79
5	33.97	2376.98	1.88
Avg	33.25	2318.52	1.82
SD	0.93	47.13	0.05

Table C.31 Mechanical properties in MD of PLA/PEPG 7 wt%

No.	Tensile strength (MPa)	Tensile modulus (MPa)	Elongation at break (%)
1	39.43	2365.93	80.32
2	37.44	2399.96	77.67
3	40.1	2452.81	82.45
4	40.22	2344.55	81.5
5	38.55	2266.18	75.8
Avg	39.15	2365.89	79.55
SD	1.04	61.83	2.47

Table C.32 Mechanical properties in TD of PLA/PEPG 7 wt%

No.	Tensile strength (MPa)	Tensile modulus (MPa)	Elongation at break (%)
1	33.95	2393.69	1.82
2	33.2	2360.79	1.95
3	31.45	2242.87	2.09
4	30.92	2200.35	1.89
5	32.02	2276.98	2
Avg	32.31	2294.94	1.95
SD	1.12	72.21	0.09

Table C.33 Mechanical properties in MD of PLA/PPG(2000) 3 wt%

No.	Tensile strength (MPa)	Tensile modulus (MPa)	Elongation at break (%)
1	46.76	2460.03	13.50
2	45.56	2494.05	14.20
3	46.91	2490.44	15.10
4	46.71	2564.38	14.70
5	43.23	2479.1	13.97
Avg	45.83	2497.60	14.29
SD	1.39	35.43	0.56

Table C.34 Mechanical properties in TD of PLA/PPG(2000) 3 wt%

No.	Tensile strength (MPa)	Tensile modulus (MPa)	Elongation at break (%)
1	30.76	2255.76	2.38
2	30.48	2390.42	2.23
3	29.67	2410.00	1.82
4	28.93	2356.84	1.98
5	29.08	2456.84	1.94
Avg	29.78	2373.97	2.07
SD	0.73	67.38	0.20

Table C.35 Mechanical properties in MD of PLA/PPG(2000) 5 wt%

No.	Tensile strength (MPa)	Tensile modulus (MPa)	Elongation at break (%)
1	36.87	2192.87	70.43
2	36.13	2164.11	73.3
3	36.04	2102.8	68.95
4	36.75	2135.46	71.54
5	36.66	2109.57	70.87
Avg	36.49	2140.96	71.02
SD	0.34	33.77	1.42

Table C.36 Mechanical properties in TD of PLA/PPG(2000) 5 wt%

No.	Tensile strength (MPa)	Tensile modulus (MPa)	Elongation at break (%)
1	18.46	1913.57	5.51
2	17.89	1890.14	4.31
3	18.19	1900.38	5.4
4	18.61	1984.32	5.69
5	18.35	1905.38	4.4
Avg	18.30	1918.76	5.06
SD	0.25	33.65	0.59

Table C.37 Mechanical properties in MD of PLA/PPG(2000) 7 wt%

No.	Tensile strength (MPa)	Tensile modulus (MPa)	Elongation at break (%)
1	29.88	2056.41	95.43
2	30.36	2090.38	98.02
3	30.22	2027.56	93.45
4	29.86	2030.67	94.9
5	29.52	1994.34	97
Avg	29.97	2039.87	95.76
SD	0.30	32.04	1.60

Table C.38 Mechanical properties in TD of PLA/PPG(2000) 7 wt%

No.	Tensile strength (MPa)	Tensile modulus (MPa)	Elongation at break (%)
1	14.73	1865.36	7.38
2	14.21	1807.06	7.93
3	14.6	1887.11	8.16
4	14.82	1896.9	6.7
5	16.76	1895.78	7.33
Avg	15.02	1870.44	7.50
SD	0.89	33.65	0.51

Table C.39 Mechanical properties in MD of PLA/Sebacic acid 3 wt%

No.	Tensile strength (MPa)	Tensile modulus (MPa)	Elongation at break (%)
1	47.29	2432.48	3.03
2	46.58	2530.34	2.49
3	45.21	2429.63	2.3
4	48.55	2603.36	2.39
5	47.73	2585.09	2.13
Avg	47.07	2516.18	2.47
SD	1.13	73.55	0.30

Table C.40 Mechanical properties in TD of PLA/Sebacic acid 3 wt%

No.	Tensile strength (MPa)	Tensile modulus (MPa)	Elongation at break (%)
1	33.06	2426.9	1.34
2	35.41	2383.86	1.49
3	34.22	2405.38	1.33
4	34.56	2495.68	1.39
5	33.53	2482.64	1.21
Avg	34.16	2438.89	1.35
SD	0.82	43.44	0.09

Table C.41 Mechanical properties in MD of PLA/Sebacic acid 5 wt%

No.	Tensile strength (MPa)	Tensile modulus (MPa)	Elongation at break (%)
1	39.35	2300.45	4.32
2	41.11	2405.5	3.67
3	42.61	2445.78	2.86
4	40.06	2366.24	2.47
5	37.36	2208.76	2.79
Avg	40.10	2345.35	3.22
SD	1.75	83.44	0.68

Table C.42 Mechanical properties in TD of PLA/Sebacic acid 5 wt%

No.	Tensile strength (MPa)	Tensile modulus (MPa)	Elongation at break (%)
1	32.38	2100.45	1.71
2	29.35	2058.5	1.35
3	33.5	2145.78	1.54
4	34.53	2266.24	1.67
5	34.38	2218.16	1.63
Avg	32.83	2157.83	1.58
SD	1.90	75.76	0.13

Table C.43 Mechanical properties in MD of PLA/Sebacic acid 7 wt%

No.	Tensile strength (MPa)	Tensile modulus (MPa)	Elongation at break (%)
1	49.15	2589.59	3.39
2	43.95	2356.62	3.13
3	46.56	2463.46	5.49
4	51.36	2685.66	3.31
5	49.99	2601.62	3.83
Avg	48.20	2539.39	3.83
SD	2.64	115.72	0.86

Table C.44 Mechanical properties in TD of PLA/Sebacic acid 7 wt%

No.	Tensile strength (MPa)	Tensile modulus (MPa)	Elongation at break (%)
1	35.61	2400.65	1.7
2	32.12	2205.5	1.74
3	35.29	2387.78	1.74
4	31.86	2166.24	1.8
5	34.27	2353.43	1.65
Avg	33.83	2302.72	1.73
SD	1.57	97.44	0.05

Table C.45 Mechanical properties in MD of PLA/Dodecanedioic acid 3 wt%

No.	Tensile strength (MPa)	Tensile modulus (MPa)	Elongation at break (%)
1	45.67	2532.48	3.33
2	44.71	2430.01	2.09
3	42.21	2209.6	2.11
4	46.11	2543.36	2.19
5	43.89	2385.09	2.1
Avg	44.52	2420.11	2.36
SD	1.39	121.21	0.48

Table C.46 Mechanical properties in TD of PLA/Dodecanedioic acid 3 wt%

No.	Tensile strength (MPa)	Tensile modulus (MPa)	Elongation at break (%)
1	31.89	2276.91	1.46
2	32.41	2303.89	1.4
3	31.52	2225.38	1.58
4	33.56	2412.34	1.21
5	33.87	2465.65	1.45
Avg	32.65	2336.83	1.42
SD	0.92	88.76	0.12

Table C.47 Mechanical properties in MD of PLA/Dodecanedioic acid 5 wt%

No.	Tensile strength (MPa)	Tensile modulus (MPa)	Elongation at break (%)
1	38.35	2303.31	3.98
2	40.71	2405.52	3.62
3	42.69	2478.98	2.86
4	40.02	2386.24	2.57
5	36.36	2198.95	2.21
Avg	39.63	2354.60	3.05
SD	2.15	95.84	0.66

Table C.48 Mechanical properties in TD of PLA/Dodecanedioic acid 5 wt%

No.	Tensile strength (MPa)	Tensile modulus (MPa)	Elongation at break (%)
1	31.38	2200.59	1.91
2	27.35	1958.5	1.28
3	30.51	2145.78	1.43
4	31.53	2272.24	1.38
5	30.38	2118.19	1.11
Avg	30.23	2139.06	1.42
SD	1.51	104.50	0.27

Table C.49 Mechanical properties in MD of PLA/Dodecanedioic acid 7 wt%

No.	Tensile strength (MPa)	Tensile modulus (MPa)	Elongation at break (%)
1	51.56	2629.07	4.38
2	47.01	2500.42	2.13
3	46.85	2463.46	3.59
4	45.63	2385.22	3.51
5	47.77	2531.41	2.89
Avg	47.76	2501.92	3.30
SD	2.02	80.17	0.75

Table C.50 Mechanical properties in TD of PLA/Dodecanedioic acid 7 wt%

No.	Tensile strength (MPa)	Tensile modulus (MPa)	Elongation at break (%)
1	33.21	2305.11	1.7
2	30.01	2105.52	1.74
3	30.25	2137.87	1.74
4	31.85	2266.24	1.8
5	34.27	2373.43	1.65
Avg	31.92	2237.63	1.73
SD	1.65	101.21	0.05

Table C.51 Mechanical properties in MD of PLA/PPG(1200) 5 wt%/M$_3$T 1 wt%

No.	Tensile strength (MPa)	Tensile modulus (MPa)	Elongation at break (%)
1	40.27	2350.85	94.61
2	40.12	2337.79	91.36
3	41.31	2406.27	86.24
4	43.01	2434.48	92.79
5	44.11	2507.96	94.03
Avg	41.76	2407.47	91.81
SD	1.56	61.47	3.00

Table C.52 Mechanical properties in TD of PLA/PPG(1200) 5 wt%/M$_3$T 1 wt%

No.	Tensile strength (MPa)	Tensile modulus (MPa)	Elongation at break (%)
1	32.21	2213.57	32.98
2	32.38	2250.14	31.08
3	33.16	2290.88	27.14
4	32.36	2245.30	28.88
5	33.28	2300.38	28.91
Avg	32.68	2260.05	29.80
SD	0.45	31.79	2.02

Table C.53 Mechanical properties in MD of PLA/PPG(1200) 5 wt%/M$_3$T 3 wt%

No.	Tensile strength (MPa)	Tensile modulus (MPa)	Elongation at break (%)
1	46.62	2534.62	84.75
2	47.84	2640.75	84.34
3	45.78	2487.49	76.16
4	47.87	2679.37	81.98
5	46.85	2546.26	82.08
Avg	46.99	2577.70	81.86
SD	0.79	71.13	3.07

Table C.54 Mechanical properties in TD of PLA/PPG(1200) 5 wt%/M$_3$T 3 wt%

No.	Tensile strength (MPa)	Tensile modulus (MPa)	Elongation at break (%)
1	33.29	2282.77	2.69
2	34.54	2387.06	2.59
3	33.29	2282.77	2.22
4	34.69	2397.65	2.48
5	33.51	2348.21	2.68
Avg	33.86	2339.69	2.53
SD	0.62	49.31	0.17

Table C.55 Mechanical properties in MD of PLA/PPG(1200) 5 wt%/M$_3$T 5 wt%

No.	Tensile strength (MPa)	Tensile modulus (MPa)	Elongation at break (%)
1	38.37	2283.86	43.63
2	36.1	2229.16	39.07
3	34.06	2208.67	40.15
4	33.11	2153.91	40.05
5	33.95	2176.27	35.34
Avg	35.12	2210.37	39.65
SD	1.90	44.96	2.65

Table C.56 Mechanical properties in TD of PLA/PPG(1200) 5 wt%/M$_3$T 5 wt%

No.	Tensile strength (MPa)	Tensile modulus (MPa)	Elongation at break (%)
1	23.83	2005.98	2.57
2	23.25	2000.01	2.43
3	24.89	2108.89	2.38
4	25.66	2178.65	2.66
5	26.94	2234.33	2.88
Avg	24.91	2105.57	2.58
SD	1.31	92.73	0.18

Table C.57 Mechanical properties in MD of PLA/PPG(1200) 5 wt%/HT(OH)$_2$ 1 wt%

No.	Tensile strength (MPa)	Tensile modulus (MPa)	Elongation at break (%)
1	44.54	2433.07	29.37
2	41.38	2394.47	25.49
3	43.19	2387.7	27.61
4	43.38	2497.19	27.53
5	42.95	2516.77	22.38
Avg	43.09	2445.84	26.48
SD	1.01	52.63	2.39

Table C.58 Mechanical properties in TD of PLA/PPG(1200) 5 wt%/HT(OH)$_2$ 1 wt%

No.	Tensile strength (MPa)	Tensile modulus (MPa)	Elongation at break (%)
1	31.46	2243.57	2.46
2	31.13	2163.14	2.12
3	31.25	2200.38	2.26
4	32.06	2294.32	2.25
5	31.19	2180.38	2.22
Avg	31.42	2216.36	2.26
SD	0.34	47.33	0.11

Table C.59 Mechanical properties in MD of PLA/PPG(1200) 5 wt%/HT(OH)$_2$ 3 wt%

No.	Tensile strength (MPa)	Tensile modulus (MPa)	Elongation at break (%)
1	49.73	2561.15	27.9
2	46.75	2699.87	23
3	45.01	2621.34	20.27
4	52.75	2768.43	28.99
5	48.9	2629.49	25.24
Avg	48.63	2656.06	25.08
SD	2.64	71.37	3.19

Table C.60 Mechanical properties in TD of PLA/PPG(1200) 5 wt%/HT(OH)$_2$ 3 wt%

No.	Tensile strength (MPa)	Tensile modulus (MPa)	Elongation at break (%)
1	36.18	2455.03	2.01
2	35.81	2334.46	2.83
3	35.18	2300.38	1.93
4	34.4	2244.30	2.11
5	34.51	2279.38	1.76
Avg	35.22	2322.71	2.13
SD	0.70	72.35	0.37

Table C.61 Mechanical properties in MD of PLA/PPG(1200) 5 wt%/HT(OH)$_2$ 5 wt%

No.	Tensile strength (MPa)	Tensile modulus (MPa)	Elongation at break (%)
1	37.9	2353.96	8.45
2	38.52	2404.34	9.84
3	36.86	2309.7	9.49
4	36	2329.03	11.23
5	33.45	2206.01	12.45
Avg	36.55	2320.61	10.29
SD	1.77	65.49	1.40

Table C.62 Mechanical properties in TD of PLA/PPG(1200) 5 wt%/HT(OH)$_2$ 5 wt%

No.	Tensile strength (MPa)	Tensile modulus (MPa)	Elongation at break (%)
1	28.02	2140.87	2.11
2	28.44	2163.14	1.87
3	28.05	2130.38	1.67
4	28.24	2164.67	1.99
5	27.77	2100.38	1.81
Avg	28.10	2139.89	1.89
SD	0.22	23.69	0.15

Appendix D

Interlayer spacing calculation

The interlayer spacing of the layer silicate in PLA/clay nanocomposite films was calculated using the Bragg's equation that is shown below.

$$2d\sin\theta = n\lambda$$

Where

λ = The wavelength of the X-ray radiation, 1.542 Å

d = The spacing between diffractional lattice planes

θ = The measured diffraction angle

n = Peaks corresponding to the basal reflection (n=1)

Diffraction angle of organoclay powder and nanocomposite films was determined by X-ray diffraction (XRD). For example, 2θ peak of MMT was 7.03^{o} which interlayer spacing of organoclay can be calculated as follow.

$$2d\sin(7.03/2) = (1)(1.542)$$

$$d = 12.5\ \text{Å}$$

Table D.1 Diffraction peak and interlayer spacing of pristine clay, organoclay and PLA/clay nanocomposite films

Sample	**2θ (^{o})**	**Interlayer spacing (nm)**
MMT	7.03^o	1.25
MMT/HT(OH)$_2$	4.47^o	1.97
	6.78^o	1.30
PLA/MMT/HT(OH)$_2$ 1% film	5.30^o	1.66
PLA/MMT/HT(OH)$_2$ 3% film	4.58^o	1.92
PLA/MMT/HT(OH)$_2$ 5% film	4.78^o	1.84
MMT/M$_3$T	2.17^o	4.06
	4.69^o	1.89
	6.67^o	1.32
PLA/MMT/M$_3$T 1% film	2.11^o	4.16
	4.35^o	2.03
	6.62^o	1.34
PLA/MMT/M$_3$T 3% film	2.15^o	4.10
	4.43^o	1.99
	6.65^o	1.33
PLA/MMT/M$_3$T 5% film	2.10^o	4.21
	4.49^o	1.97
	6.74^o	1.31

Appendix E

Data of optical properties

Table E.1 Optical transmittance of pristine clay, organoclay and PLA/clay nanocomposite films

Sample	PLA/PPG 5 wt%	PLA/MMT/HT(OH)$_2$ films			PLA/MMT/M$_3$T films		
		1 wt%	3 wt%	5 wt%	1 wt%	3 wt%	5 wt%
1	63.48	47.90	43.52	43.32	54.13	49.87	46.06
2	65.61	45.75	44.91	45.96	56.06	48.40	47.82
Avg	64.55	46.83	44.22	44.64	55.10	49.14	46.94
SD	1.06	1.07	0.69	1.32	0.97	0.74	0.88

Appendix F

Data of barrier properties

Table F.1 Oxygen permeation (cc.mil/(m^2.day.atm)) of nanocomposite films at different organoclay loading

Sample	**PLA/PPG 5 wt%**	**PLA/MMT/HT(OH)$_2$ films**			**PLA/MMT/M$_3$T films**		
		1 wt%	3 wt%	5 wt%	1 wt%	3 wt%	5 wt%
1	799.18	640.09	575.00	745.55	666.54	625.50	750.51
2	805.65	648.40	578.98	752.10	663.12	630.21	748.09
3	800.43	635.21	583.22	741.33	675.43	632.89	756.30
4	795.07	638.67	585.30	743.65	675.00	633.48	751.77
Avg	800.08	640.59	580.63	745.66	670.02	630.52	751.67
SD	4.36	5.59	4.58	4.63	6.16	3.64	3.45

Table F.2 Water vapor permeation (gm.mil/(m^2.day.atm)) of nanocomposite films at different organoclay loading

Sample	**PLA/PPG 5 wt%**	**PLA/MMT/HT(OH)$_2$ films**			**PLA/MMT/M$_3$T films**		
		1 wt%	3 wt%	5 wt%	1 wt%	3 wt%	5 wt%
1	254.62	211.45	211.91	220.15	200.92	195.21	216.81
2	260.43	218.78	206.00	225.33	198.00	196.94	221.22
3	257.87	219.32	213.11	222.41	202.59	199.01	224.55
4	258.98	220.17	209.88	228.67	196.34	197.55	220.07
Avg	257.98	217.43	210.23	224.14	199.46	197.18	220.66
SD	2.47	4.03	3.12	3.69	2.82	1.57	3.19

VITA

Mr. Poom Boonfaung was born in Suratthani, Thailand on February 17, 1986. He completed high school at Suratthani School, Thailand in 2005 and received the Bachelor's Degree from Department of Chemical Engineering, Faculty of Engineering, King Mongkut's University of Technology Thonburi, Thailand in 2009. He continued his study for Master's Degree in Chemical Engineering at the Department of Chemical Engineering, Faculty of Engineering, Chulalongkorn University in June, 2009.

In addition, he was invited for oral presentation in Pure and Applied Chemistry International Conference 2011. This conference was held during 5-7 January, 2011 at Bangkok, Thailand.